

AD-A215 769

NAVAL POSTGRADUATE SCHOOL

Monterey, California

2

DTIC
ELECTE
DEC 26 1989
D C D



THESIS

AN ANALYSIS OF DIURNAL WIND VARIABILITY
IN THE SANTA BARBARA CHANNEL
FROM SODAR MEASUREMENTS

by

Douglas H. Scovil, Jr.

June 1989

Thesis Advisor:

William J. Shaw

Approved for public release; distribution is unlimited

0 1 0

REPORT DOCUMENTATION PAGE				Form Approved GMB No 0704 0188	
1a REPORT SECURITY CLASSIFICATION Unclassified			1b RESTRICTIVE MARKINGS		
2a SECURITY CLASSIFICATION AUTHORITY			3 DISTRIBUTION AVAILABILITY OF REPORT Approved for public release; distribution is unlimited		
2b DECLASSIFICATION/DOWNGRADING SCHEDULE					
4 PERFORMING ORGANIZATION REPORT NUMBER(S)			5 MONITORING ORGANIZATION REPORT NUMBER(S)		
6a NAME OF PERFORMING ORGANIZATION Naval Postgraduate School		6b OFFICE SYMBOL (if applicable) 63		7a NAME OF MONITORING ORGANIZATION Naval Postgraduate School	
6c ADDRESS (City, State, and ZIP Code) Monterey, California 93943-5000		7b ADDRESS (City, State, and ZIP Code) Monterey, California 93943-5000			
8a NAME OF FUNDING SPONSORING ORGANIZATION		8b OFFICE SYMBOL (if applicable)		9 PROGRAM ELEMENT, REPORT IDENTIFICATION, MARK	
8c ADDRESS (City, State, and ZIP Code)		10 SOURCE OF FUNDING NUMBERS			
		PROGRAM ELEMENT NO		PROJECT NO	TASK NO
				WORK UNIT ACCESSION NO	
11 TITLE (Include Security Classification) AN ANALYSIS OF DIURNAL WIND VARIABILITY IN THE SANTA BARBARA CHANNEL FROM SODAR MEASUREMENTS					
12 PERSONAL AUTHOR Scovil, Douglas H., Jr.					
13a TYPE OF REPORT Master's thesis		13b TIME COVERED FROM _____ TO _____		14 DATE OF REPORT (Year, Month, Day) 1989 June	
				15 PAGE COUNT 84	
16 SUPPLEMENTARY NOTES The views expressed in this thesis are those of the author and do not reflect the official policy or position of the Department of Defense or the U.S. Government					
17 CRYPTO CODES		18 SUBJECT TERMS (Continue on reverse if necessary and identify by block number)			
FIELD	GROUP	Diurnal wind variability, SODAR system, Power Density Spectra, Santa Barbara Channel			
19 ABSTRACT (Continue on reverse if necessary and identify by block number) Diurnal wind variability within the atmospheric boundary layer along the coast of the Santa Barbara Channel is studied by spectral analysis of SODAR (Sound Detection and Ranging) wind measurements. Rotary spectral analysis is used to investigate wind circulations and oscillations in the vertical. Power density spectral analysis is used to find frequencies with the greatest amount of kinetic energy. The results show a tendency for counterclockwise rotation in the lowest level and clockwise rotation in the upper levels. Some case show counterclockwise rotation in all levels. Most of the kinetic energy was concentrated at a diurnal frequency related to local sea and land breezes. However, a secondary kinetic energy maximum is consistently found at a sub-diurnal frequency. The source of this sub-diurnal energy in the vertical may be a mesoscale circulation, such as the Gaviota Eddy or the Catalina Eddy.					
20 DISTRIBUTION STATEMENT OF ABSTRACT <input checked="" type="checkbox"/> UNCLASSIFIED <input type="checkbox"/> CONFIDENTIAL <input type="checkbox"/> SECRET				21 ABSTRACT SECURITY CLASSIFICATION	
22 AUTHOR (Last Name, First Name, Middle Initial) W. J. Shaw				23 PERFORMING ORGANIZATION (Include Area Code) 408-646-2516	
				24 REPORT NUMBER 63	

Approved for public release; distribution is unlimited

An Analysis of Diurnal Wind Variability
in the Santa Barbara Channel
from SODAR Measurements

by

Douglas H. Scovil, Jr.
Lieutenant, United States Navy
B. S., U. S. Naval Academy, 1980

Submitted in partial fulfillment of the
requirements for the degree of

MASTER OF SCIENCE IN METEOROLOGY AND PHYSICAL OCEANOGRAPHY

from the

NAVAL POSTGRADUATE SCHOOL
June 1989

Author:

Douglas H. Scovil, Jr.
Douglas H. Scovil, Jr.

Approved by:

William J. Shaw
William J. Shaw, Thesis Advisor

Kenneth L. Davidson
Kenneth L. Davidson, Second Reader

Robert J. Renard
Robert J. Renard, Chairman,
Department of Meteorology

Gordon E. Schacher
Gordon E. Schacher,
Dean of Science and Engineering

ABSTRACT

Diurnal wind variability within the atmospheric boundary layer along the coast of the Santa Barbara Channel is studied by spectral analysis of SODAR (Sound Detection and Ranging) wind measurements. Rotary spectral analysis is used to investigate wind circulations and oscillations in the vertical. Power density spectral analysis is used to find frequencies with the greatest amount of kinetic energy. The results show a tendency for counterclockwise rotation in the lowest level and clockwise rotation in the upper levels. Some cases show counterclockwise rotation in all levels. Most of the kinetic energy was concentrated at a diurnal frequency related to local sea and land breezes. However, a secondary kinetic energy maximum is consistently found at a sub-diurnal frequency. The source of this sub-diurnal energy in the vertical may be a mesoscale circulation, such as the Gaviota Eddy or the Catalina Eddy.

Accession	
NTIS	<input checked="" type="checkbox"/>
DTIC	<input type="checkbox"/>
Unannounced	<input type="checkbox"/>
Justification	
By	
Distribution	
Availability	
Dist	
A-1	

TABLE OF CONTENTS

I.	INTRODUCTION.....	1
A.	The Atmospheric Boundary Layer and its Operational Effects	2
B.	The Influence of Eastern North Pacific Climatology	5
C.	The Coastal Atmospheric Boundary Layer	7
D.	The Atmospheric Boundary Layer in the Santa Barbara Channel	10
II.	DATA COLLECTION AND ANALYSIS PROCEDURES	14
A.	The Sodar System	14
B.	Measurement Site	15
C.	Treatment of the Data	16
D.	Evaluation of Time Series	19
E.	Spectral Analysis of the Data	26
III.	PRESENTATION OF RESULTS	29
A.	Evaluation of the Low Level Wind Field During SCCCAMP	29
B.	Power Density Spectra of the U-Component	40
C.	Power Density Spectra of the V-Component	49
D.	Rotary Spectra	59
E.	Discussion of Results	64
IV.	SUMMARY	71
A.	Review of Analysis Procedures	71
B.	Conclusions	72
C.	Areas for Future Research	72

LIST OF REFERENCES	75
INITIAL DISTRIBUTION LIST	77

ACKNOWLEDGMENTS

I wish to extend sincere thanks to my advisor, Associate Professor W. J. Shaw and my second reader, Professor K. L. Davidson. Without their guidance and review, this thesis could not have been completed. I would like to express sincere gratitude to Associate Professor Shaw for all of the time he spent helping me with FORTRAN code, interpreting results and many hours of valuable advice. This thesis is dedicated to my wife, U Son, and my daughter, Sharon, whose understanding, patience and support sustained me during a very challenging period.

I. INTRODUCTION

The Naval Postgraduate School participated in the South Central Coast Cooperative Aerometric Monitoring Program (SCCCAMP) experiment, which was conducted within the Santa Barbara Channel during the fall of 1985. The SCCCAMP field measurements were intended to appraise the significance of several processes: the local recirculation of pollutants including the diurnal sea and land breeze cycle, return offshore flow from mountain ridges, surface and upper-level transport from Los Angeles and the transport and transformation of shoreline and near-offshore pollutants (Dabberdt, 1984).

The data collected during the SCCCAMP experiment included four main categories of measurements, each of which used differing types of collection platforms. Upper-air meteorological measurements from six rawinsondes and a network of twelve doppler acoustic sounders were used to describe mesoscale and microscale features respectively. Surface meteorological and air quality measurements were collected from a network of 40 surface wind monitoring stations. These were located aboard the research vessel Acania, on deep water buoys, on offshore platform stations and at shore stations. Boundary layer aerometric and

aerochemetric measurements were collected by two meteorological research aircraft, three aerometric aircraft and one laser radar (LIDAR) equipped aircraft. Finally, data were collected from transport-tracer experiments, using three perfluorocarbon compounds as tracers and an electron-capture gas chromatograph to measure atmospheric sample concentrations released from shore stations, the research vessel Acania and a single aircraft. (Dabberdt, 1984)

The portion of the SCCAMP data used for this thesis was collected by a sodar (sound detection and ranging) station near Goleta, California. The purpose of this thesis is to use the sodar data to investigate diurnal atmospheric boundary layer wind structure along the northern coast of the Santa Barbara Channel. The rotational and kinematic characteristics of the wind field will be examined, using spectral analysis to determine the existence and frequency of any prevalent or well defined circulations or oscillations. This thesis will also consider how synoptic weather patterns and local topography relate to the observations.

A. THE ATMOSPHERIC BOUNDARY LAYER AND ITS OPERATIONAL EFFECTS

The part of the atmosphere extending from the surface up to the upper limit of frictional influence of the earth's surface, or geostrophic wind level, is known as the

atmospheric boundary layer (ABL). The upper limit of the ABL is generally marked by a subsidence inversion, a type of temperature inversion produced by adiabatic warming of a layer of subsiding air. Vertical changes of mean temperature, humidity and wind at the surface and in the inversion are much larger than horizontal changes. Turbulence in the ABL reduces the vertical changes of these variables between the surface and inversion.

The ABL is generally divided into sub-layers based on the characteristics of its vertical structure. The layer within the lower ten percent of the ABL is known as the surface layer. It is a region of strong vertical changes in mean quantities, and in the case of horizontally homogeneous turbulence, it is also a region where fluxes do not change appreciably with height. The remainder of the ABL above the surface layer is called the mixed layer for unstable ABL's and the intermittent layer for stable ABL's. The mixed layer is a region of nearly continuous turbulence. However, in the intermittent layer turbulence can be isolated and may not persist. (Holtslag and Nieuwstadt, 1986)

The ABL is unstable when there is an upward heat flux; the air in the surface layer is warmer than the air in the mixed layer. This produces turbulence, which mixes temperature, humidity and other variables. Conversely, a stable ABL exists when air in the surface layer is cooler

than the air in the mixed layer. This stratification results in suppressed turbulence. The stable ABL is normally an order of magnitude shallower than the unstable ABL. Over land, a stable ABL is formed by cooling due to the earth's emission of long wave radiation. Over water, a stable ABL is formed by upwelling or warm air advection aloft. (Holtslag and Nieuwstadt, 1986)

The ABL has numerous operational impacts. Changes in humidity and temperature that occur in the ABL can influence the propagation of electromagnetic (EM) forms of energy by causing changes in the index of refraction. Ducting of EM radiation can occur when humidity decreases sufficiently rapidly with height. Drier air, which exists over a land mass, can be advected over the sea surface by land breeze circulations or by the return flow of a sea breeze. This is a common cause of strong surface and elevated ducts (Beach, 1980). Resulting ducts make possible a continual downward refraction and reflection cycle of EM waves that can produce tactically significant over-the-horizon radar detection, electronic countermeasures and communications capabilities. More specifically, tactically vital systems such as fire-control and surveillance radars, radio, forward-looking infrared (FLIR) scanners and lasers probably will enjoy better performance as our knowledge of the ABL's vertical structure improves. Enhancing our

knowledge of the ABL's vertical structure may allow us to more accurately forecast phenomena which can attenuate or even eliminate tactical capabilities that rely on optimization of EM propagation. For example, absorption of aerosols associated with fog, stratus clouds, rain or haze can significantly degrade both EM and electro-optical propagation. Thus, the mesoscale wind structure and related circulations which occur within the ABL can affect a variety of naval operations in the coastal environment.

B. THE INFLUENCE OF EASTERN NORTH PACIFIC CLIMATOLOGY

During the fall season, the climate of the eastern North Pacific region is dominated by a persistent synoptic-scale feature known as the eastern Pacific subtropical anticyclone. Migratory low pressure systems form in the western and central Pacific Ocean and move east-northeastward. The low pressure systems develop as they track southward of the Aleutian Island chain, then mature and decay in the Gulf of Alaska. The region north of 40 degrees North latitude experiences the coldest surface air temperatures, the most precipitation, the highest frequency of broken or overcast cloud cover and nearly the highest relative humidity. While the eastern Pacific subtropical anticyclone keeps the storm track of migratory low pressure systems north of 40 degrees North latitude, it also dominates the climate in the area between 20 and 40 degrees North latitude. This region has

one-third to one-fifth the precipitation and nearly half the frequency of broken or overcast cloudiness of the storm track region. The area between 20 and 40 degrees North latitude also has the lowest mean relative humidity in the eastern North Pacific. (U. S. Navy , 1977)

The eastern Pacific subtropical anticyclone produces a synoptic-scale northerly flow parallel to the coast of California. When winds flow parallel to the coast, continuity of mass requires the subsurface layers of the ocean near the coast to experience compensating vertical motion (Arthur, 1965). The earth's rotation forces the transport of surface waters away from the shoreline, allowing for replacement by cooler subsurface waters (Caldwell, et. al., 1986). The result is upwelling, which cools the ABL from below and often leads to a stable stratification. Not surprisingly, the coldest sea-surface temperatures equatorward of 40 degrees North latitude are found along the coast of California. The cooler water creates a weak local pressure ridge and increases the thermal gradient between land and sea (Halpern, 1974). On the eastern edge of the eastern Pacific subtropical anticyclone, areas just inland of the coast of California are subjected to heating during the day. The coastal thermal gradient produced by daytime surface heating of the land and cooling of the sea surface by upwelling frequently results

in the formation of a sea breeze circulation (Johnson and O'Brien, 1973).

C. THE COASTAL ATMOSPHERIC BOUNDARY LAYER

The coastal ABL is affected by forcing from synoptic-scale pressure patterns, the constraining influence of topography, differential heating of the sea and land, and diabatic heating of sloping terrain near the coast. Forcing by synoptic-scale pressure gradients can have a significant effect on both atmospheric and oceanic conditions near a coast. During the Organization of Persistent Upwelling Structures (OPUS) II experiment, synoptic-scale weather patterns played a significant role in forcing mesoscale wind variability (Caldwell, et. al., 1986). Research by Caldwell, et. al. indicates that nearly 85 percent of the total temporal and spatial wind variability described by an empirical orthogonal function (EOF) analysis could be identified with synoptically induced fluctuations. The previous section of this chapter explains how synoptic-scale features like the eastern Pacific subtropical anticyclone produce subsidence inversions and upwelling, which in turn contribute to the formation of a stable ABL and sea breeze circulations.

The constraining influence of topography can also affect wind flow and vertical motion in the coastal ABL. The coastline itself is an important topographic influence in

terms of mesoscale variability. Since the sea and land surface roughnesses differ by several orders of magnitude, a contrast between over-land and over-water roughnesses exists at a coast. This controls changes in turbulence and affects wind speed and direction in the ABL (Sethuraman and Raynor, 1978). Gaps in a coastal mountain range can have a funneling effect, steering the flow of air into a relatively narrow region, such as a pass or ravine. This funneling is probable in areas dominated by a low, strong inversion because the inversion will prevent the sea breeze from flowing over a mountain range. Instead, it is forced between gaps and around the mountain range (Olsson, et. al., 1973). Finally, the amount of vegetation covering the land along a coastline can be important. All else being equal, a dry coastline with sparse vegetation will absorb more heat than a moist, foliated coastline (Atkinson, 1981). As a result, an arid coastline can quickly initiate a sea breeze circulation. Differential heating of the sea and land along a coast occurs because the sea has a higher heat capacity than the land. In a relatively clear and calm atmosphere during the daytime, solar radiation heats the land faster than it does the sea, generating a horizontal temperature gradient. The air over the land warms and becomes less dense than the air over the sea. Because the vertical decrease of pressure is directly proportional to density,

that change is greater in the cooler air over the sea than it is in the warmer air over the land. So at a constant altitude above both sea and land, the higher pressure occurs over the land, and the lower pressure occurs over the sea. This pressure gradient creates a flow of air from land to sea and produces convergence over the sea in the upper ABL. This convergence induces subsidence over the sea, which in turn causes divergence at the surface and a low-level onshore flow. The result is an upper-level flow from land to sea and a near-surface flow from sea to land. The near-surface flow from the sea is known as a sea breeze. At night, the land becomes colder than the sea and the circulation reverses itself and becomes a land breeze, with the near-surface flow from land to sea. (Atkinson, 1981)

The presence of sloping terrain near a coast can also influence conditions within the coastal ABL. An east-west oriented mountain range running parallel to a coastline provides a large slope facing the sea. An extensive southward-facing slope becomes warmer than the inland plateaus and mountains during the day (Atkinson, 1981). The air near the sloping land becomes warmer than the air in the free atmosphere above the ABL, so that pressure increases away from the slope. A horizontal pressure gradient from plateau to slope results and an upslope wind is created, enhancing the daytime sea breeze. At night, the system

reverses, resulting in a downslope drainage wind from air cooled by advection over a cold land surface. (Atkinson, 1981)

D. THE ATMOSPHERIC BOUNDARY LAYER IN THE SANTA BARBARA CHANNEL

The ABL in the Santa Barbara Channel is a coastal ABL that is affected by synoptic-scale systems, topography, differential heating between sea and land, and diurnal heating of sloping terrain. As mentioned in the previous section, analysis of the OPUS II data by Caldwell shows that 85 percent of the wind variability in the Santa Barbara Channel is due to synoptic-scale forcing. Differential heating of sea and land, and topographic influences in the Santa Barbara Channel only account for six percent and four percent of the wind variability, respectively (Caldwell, et. al., 1986). However, the OPUS II data indicate that the dominant energy in the Santa Barbara Channel is not from synoptic-scale systems, but is instead due to diurnal and topographic influences.

The Santa Barbara Channel receives synoptic-scale forcing from the eastern Pacific subtropical anticyclone, which creates northerly to northwesterly winds over the coast of southern California. These winds flow parallel to the coast between Point Arguello and Point Conception, where the direction of the coastline changes sharply from north-

south to east-west (Fig. 1). The mountainous coastal topography in this area causes cyclonic turning of the wind in the Santa Barbara Channel (Caldwell, et. al., 1986). Cyclonic turning of the wind can lead to the formation of a daytime mesoscale circulation known as the Gaviota Eddy, which extends from Point Conception to just east of Gaviota (Dabberdt, 1984). Based on a streamline analysis by Dabberdt, the Gaviota Eddy has a diameter of about 20 to 25 miles and forms between Point Conception and Gaviota (Fig. 2). Cyclonic turning of the wind also produces westerly winds in the Santa Barbara Channel that are parallel to the coast. As explained earlier, these westerly winds lead to upwelling, which frequently results in the formation of a sea breeze circulation. As discussed in the previous section, diurnal heating of sloping terrain can produce upslope and downslope winds. Along the northern coast of the Santa Barbara Channel, the Santa Ynez mountain range is east-west and provides a large sloping surface that faces equatorward. This sloping surface parallel to the coastline makes it possible for sea and land breezes in the Santa Barbara Channel to be enhanced by upslope and downslope winds, respectively.

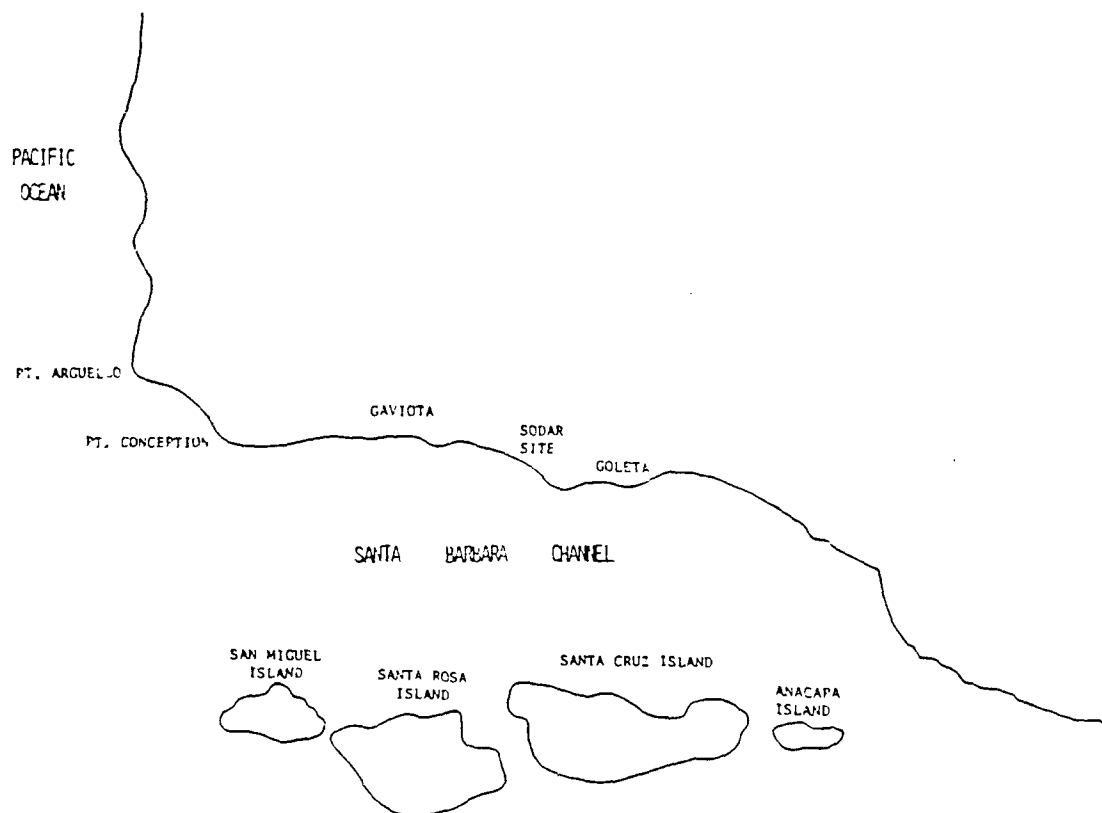


Figure 1. The Santa Barbara Channel Region

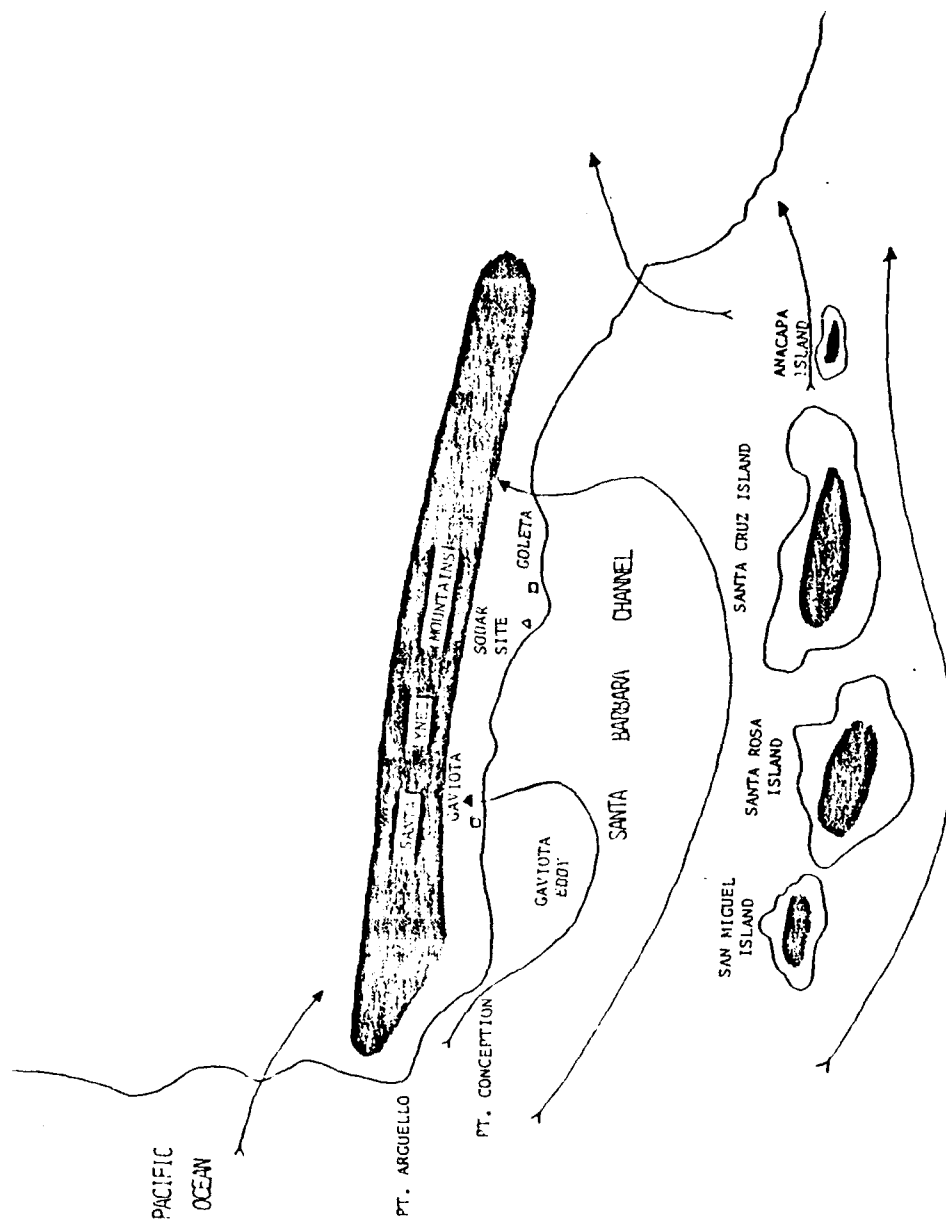


Figure 2. The Gaviota Eddy and Large Scale Topography Surrounding the Santa Barbara Channel

II. DATA COLLECTION AND ANALYSIS PROCEDURES

The data used for this thesis were collected via hourly sodar measurements over a six-week period along the northern coast of the Santa Barbara Channel. Horizontal wind components at different levels have been plotted together with inversion heights to evaluate the data quality with respect to altitude and to serve as an aid in discovering trends in the data. The basic analysis approach involves spatial and temporal extrapolation and interpolation for missing data, plus a combination of quadratic detrending of the data and fast Fourier transform (FFT) analysis to obtain rotary spectra and power density spectra. Interpretation of the plotted rotary spectra and power density spectra is then used to infer diurnal vertical wind structure and variability in the ABL.

A. THE SODAR SYSTEM

Sodar is capable of providing vertical profiles of horizontal wind vectors (Wyckoff, et. al., 1973). It operates by transmitting bursts of acoustic energy. After a burst is transmitted, the receiver is activated and its output recorded. What sodar basically does is measure the intensity of backscattered sound, which results from small

inhomogeneities in the acoustic refractive index. This allows sodar to measure the scattering structures in the ABL up to the base of the inversion. Sodar works on the principle that the intensity of backscattered sound is directly proportional to the strength of the small scale density fluctuations. Energy can be returned from a pulse of sound that is transmitted up into the atmosphere by scattering from wind velocity or air temperature gradients (McAllister, et. al., 1969). Echoes from the wind, which is a moving target, are shifted in frequency by the doppler effect. The sodar receives and measures the doppler shift along each transmission axis, yielding a wind measurement for each radial velocity.

The sodar used to collect the data analyzed in this thesis was an Echosonde III system manufactured by the Radian Corporation of Austin, Texas. It operates by emitting 2-KHz pulses of 100 ms duration in succession from three antennas. The use of three antennas permitted the three components of the velocity field to be retrieved. One axis was oriented vertically, while the other two antennas were oriented west and south at 18 degrees off zenith. (Shaw, et. al., 1986)

B. MEASUREMENT SITE

The Naval Postgraduate School sodar station was located at the foot of the Ellwood pier at 34 degrees, 25 minutes,

20 seconds North latitude and 119 degrees, 55 minutes, 43 seconds West longitude, just west of Goleta, California. A 20-meter high meteorological instrument tower was located at the head of the Ellwood pier, 450 meters from the shoreline. (Shaw, et. al., 1986) The surrounding topography is dominated by the east-west orientation of the Santa Ynez mountain range, which runs parallel to the northern coast of the Santa Barbara Channel and is only a few kilometers inland from the coastline. To the north of the Santa Ynez mountains are the Santa Ynez and Santa Maria valleys. The northern shore of the Santa Barbara Channel is almost continuously lined with bluffs. In the immediate vicinity of the head of the Ellwood pier there was a 30-meter gap between two large bluffs, which rose to a height of 30 meters and were 10 meters away from the shoreline (Fig. 3). The shore is oriented in such a way that southeasterly to southwesterly winds can reach the land on a trajectory which lies purely over water, possibly passing over the Santa Barbara Channel Islands 50 kilometers away.

C. TREATMENT OF THE DATA

The sodar data were collected during three periods of continuous system operation in 1985: from 8 to 12 September, from 21 to 29 September and from 6 to 11 October. The sodar was inoperative between 13 and 19 September. Other days of the data collection period not included in the analysis are

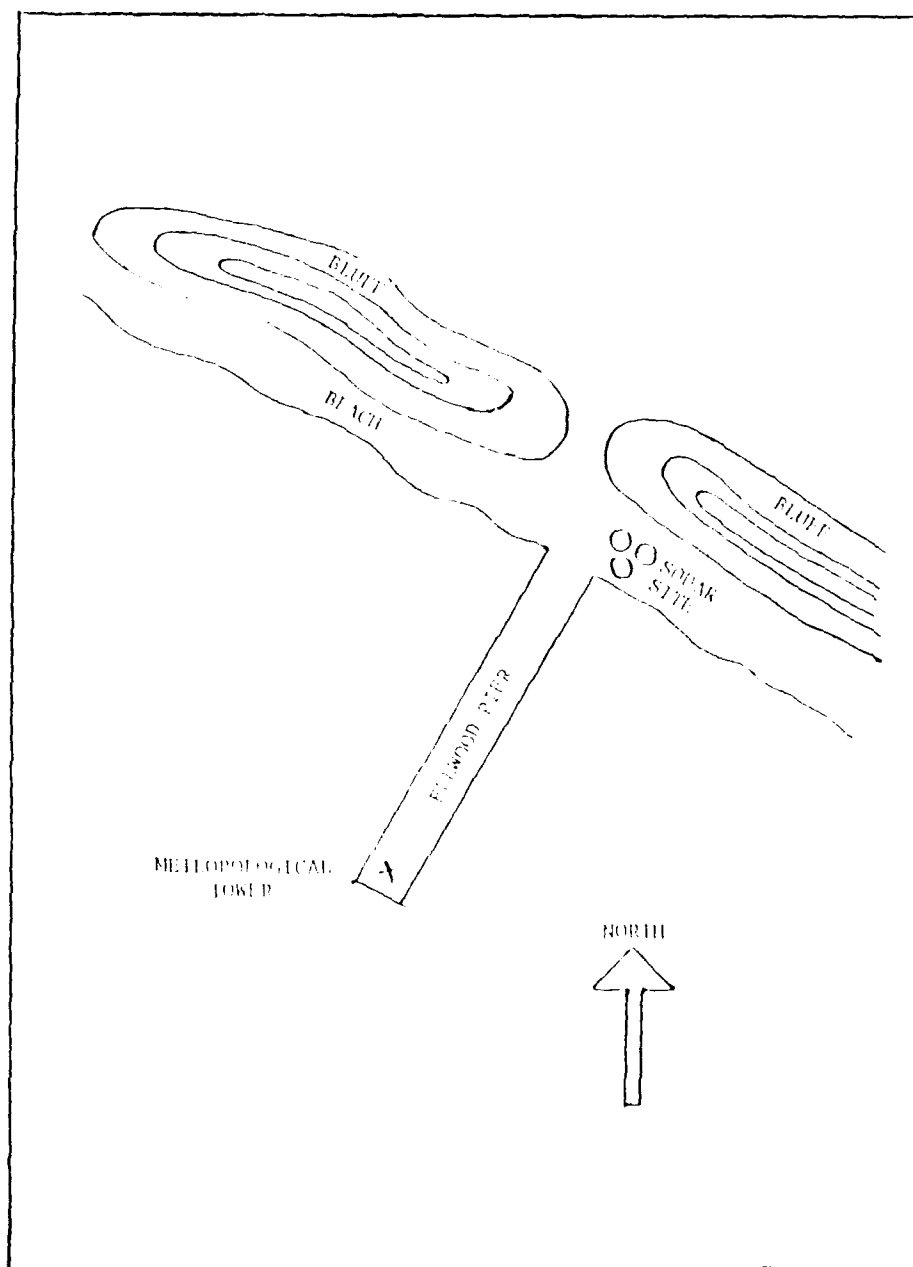


Figure 3. Local Topography near the Sodar site includes two 30 meter high bluffs located ten meters ashore, with a gap between the bluffs only a few meters from the Sodar site.

days which are missing three or more consecutive hours of data at all 20 vertical measurement levels. Since one of the main purposes of this thesis is to investigate diurnal wind structure, data gaps of three or more hours are unacceptable, because extrapolation or interpolation over a three-hour period of missing data could yield misleading results.

The data from the sodar consist of wind speeds and wind directions at 20 vertical levels over 120-, 216- and 144-hour periods, respectively. A FORTRAN computer program converted the raw data into u and v wind components and used data at adjacent heights in the vertical to linearly extrapolate or interpolate in the vertical for missing data at any given level. The computer program did not attempt to process large blocks of missing data over three or more consecutive levels. In those cases where the computer program could not vertically extrapolate or interpolate, a second computer program used the spatially adjusted data from the output of the first computer program to temporally extrapolate or interpolate for missing data at any given time. Like the first computer program, the second computer program did not attempt to process large sections of missing data over three or more consecutive hours. After both spatial and temporal extrapolation and interpolation of the raw data, there were a few blocks or groups of missing data,

but the number of these missing data were relatively small in size and number in comparison to the overall processed data. Periods which still had groups of missing data were omitted.

D. EVALUATION OF TIME SERIES

Time series of the horizontal wind components, u and v , for all twenty vertical levels, are plotted simultaneously on six plots for the periods 8-12 September, 21-29 September and 6-11 October 198. Time series of the mean horizontal wind components, u and v , and perturbation horizontal wind components, u^1 and v^1 , are individually plotted at each vertical level (Figs. 4, 5, 6, 7, 8 and 9). On the abscissa of these plots, times of 0, 24, 48, etc. correspond to midnight local standard time. From 2 to 10 hours is considered to be morning, from 10 to 18 hours is afternoon, and from 18 to 2 hours is evening. The sodar backscatter intensities were recorded on a line printer display terminal. This display was used to estimate inversion height (Shaw, et. al., 1986), which is represented on each figure by dashed lines. Examination of these figures allows us to reach several conclusions regarding the quality of the data. First, above 250 meters (or the tenth vertical level), the data become significantly less coherent with height. Second, data measured at levels above the inversion height are generally of a highly variable nature. Sodar

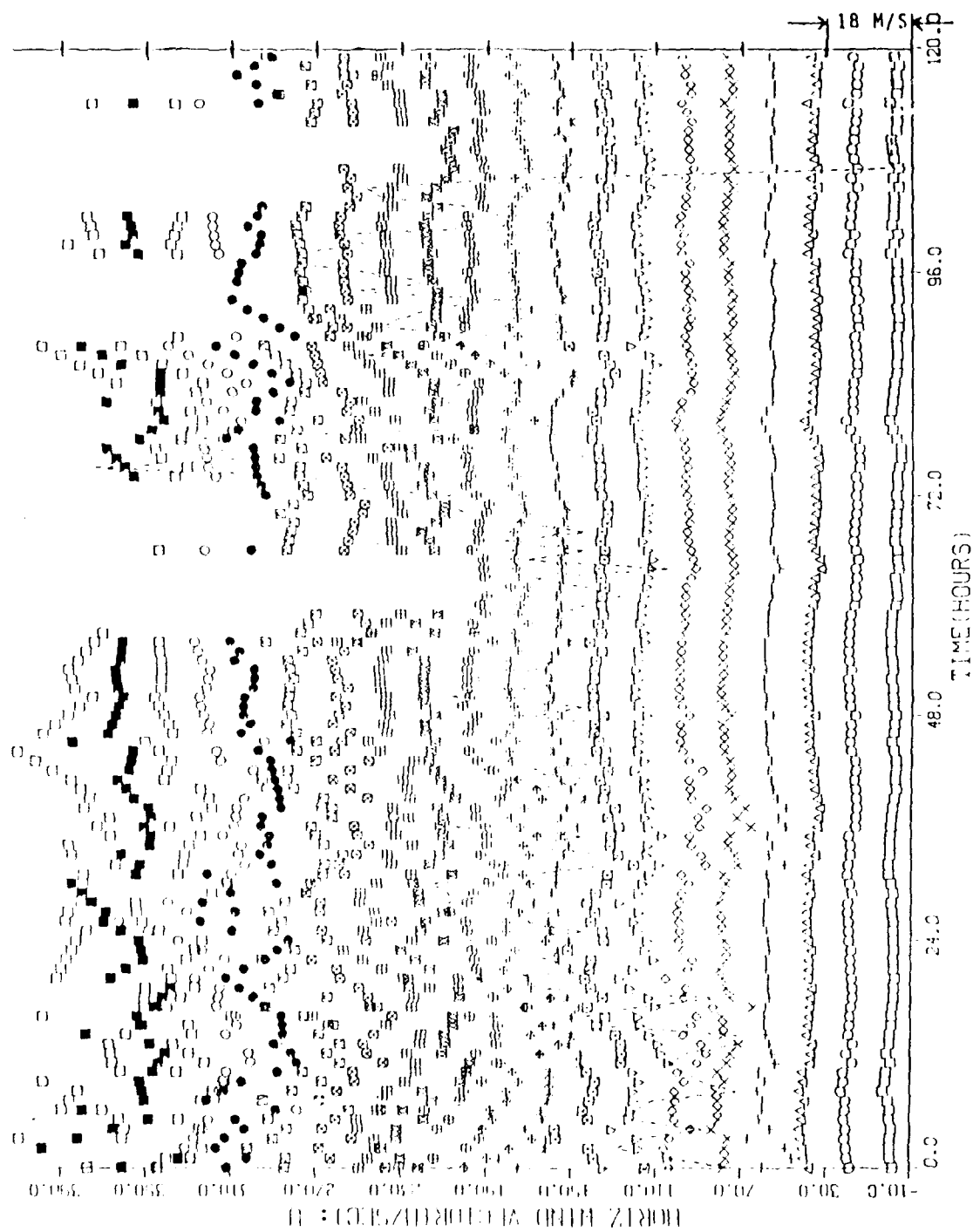


Figure 4. Horizontal Wind Vector (M/Sec): U

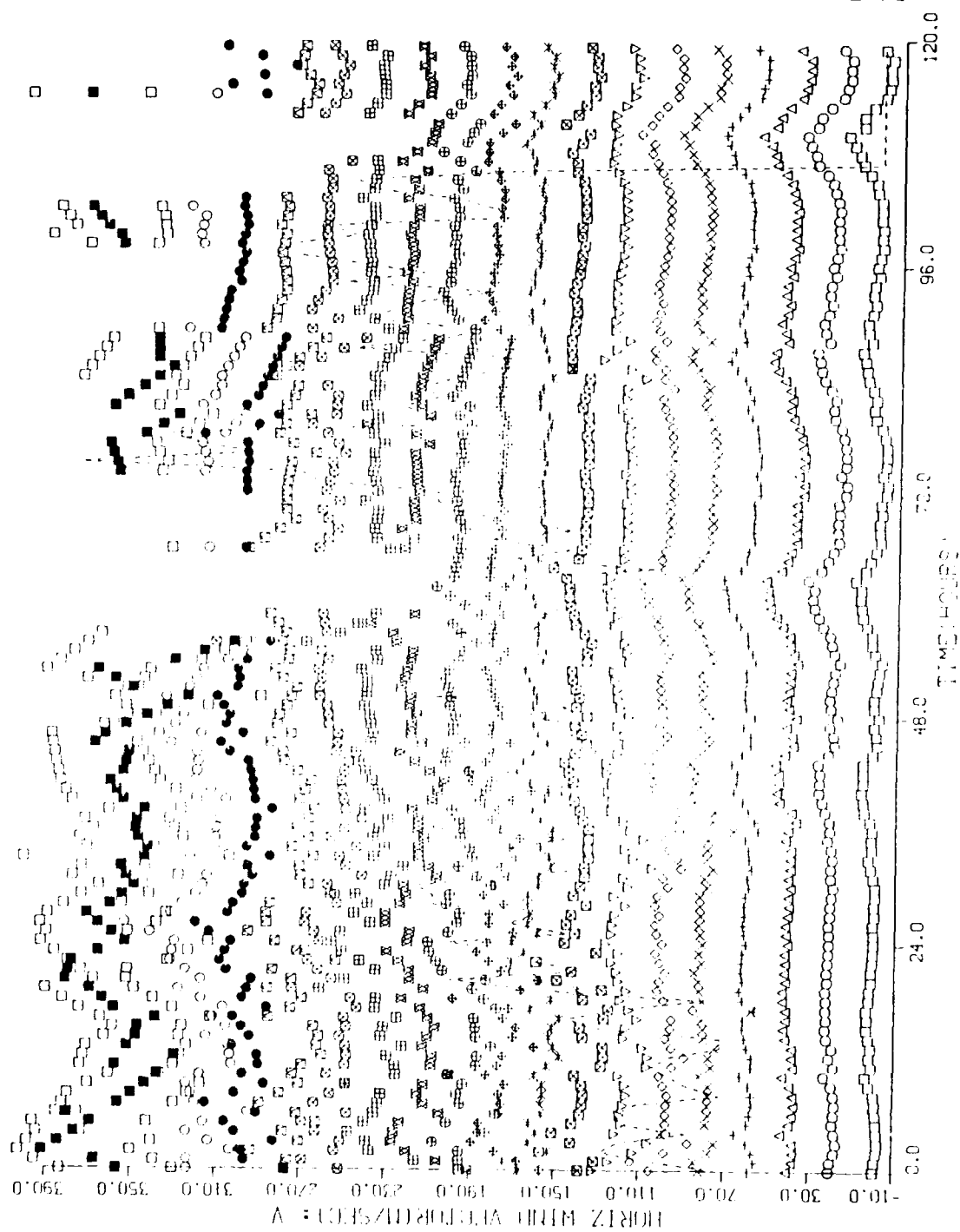


Figure 5. Horizontal Wind Vector (M/Sec): V

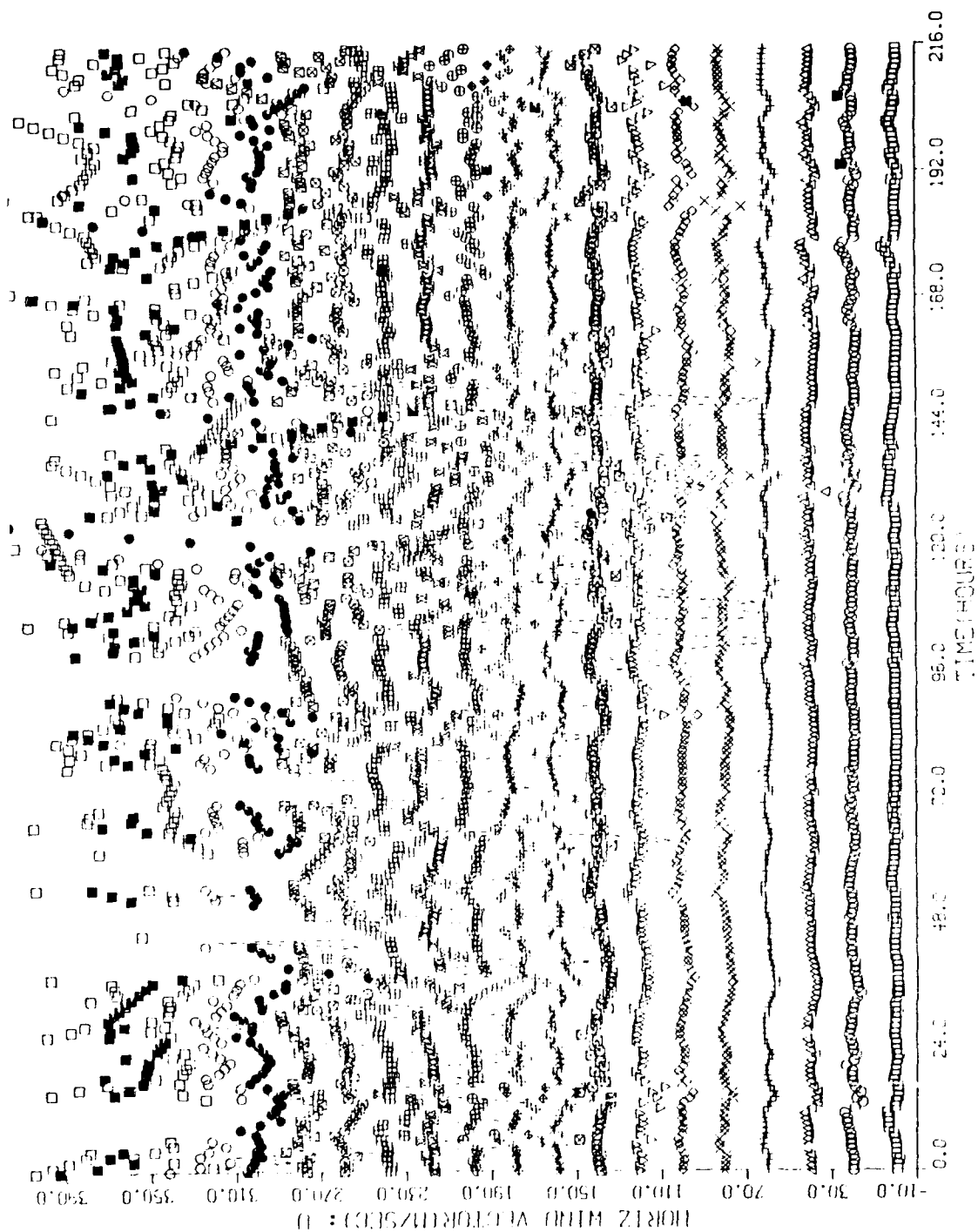


Figure 6. Horizontal Wind Vector (M/Sec): U

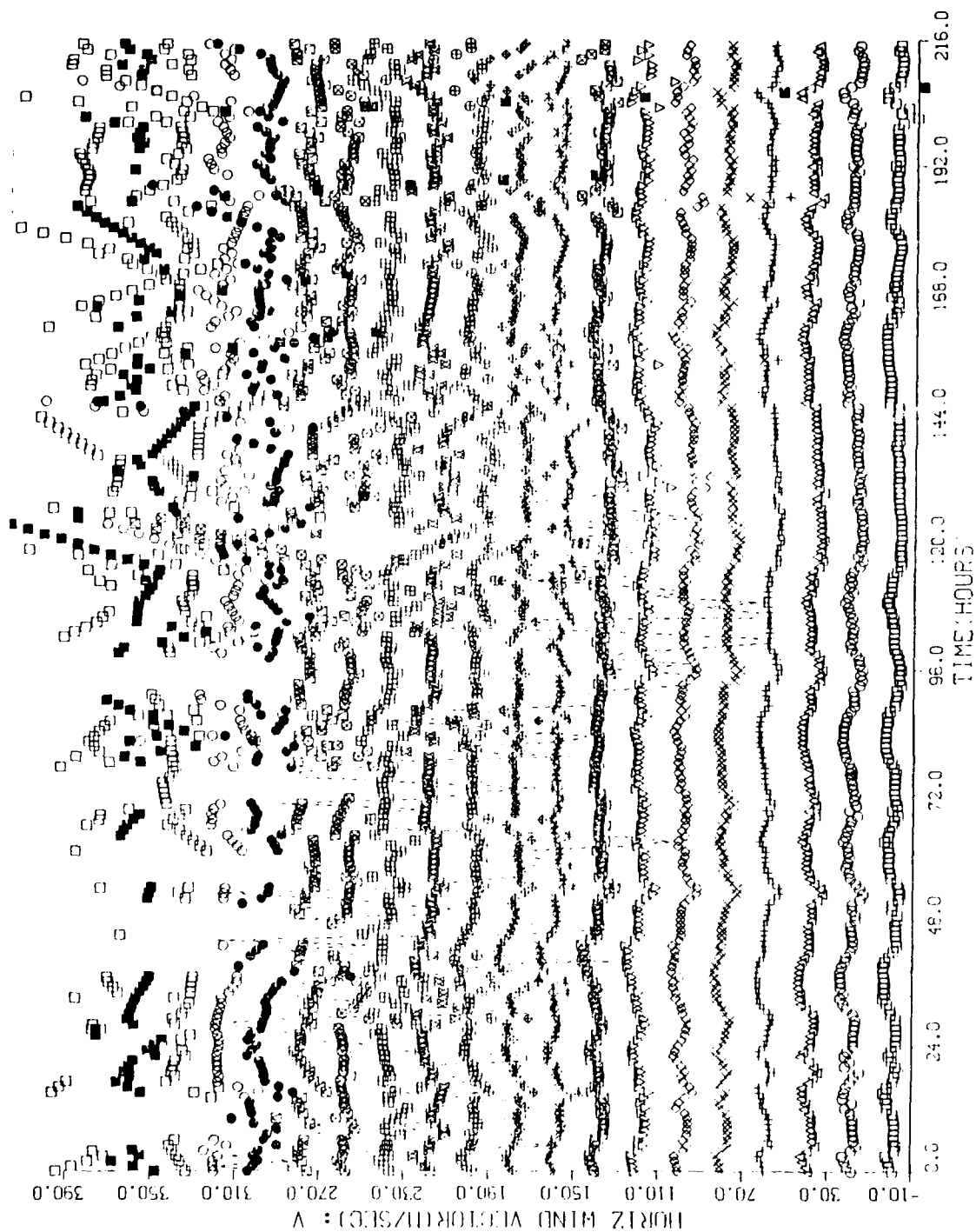


Figure 7. Horizontal Wind Vector (M/Sec): V

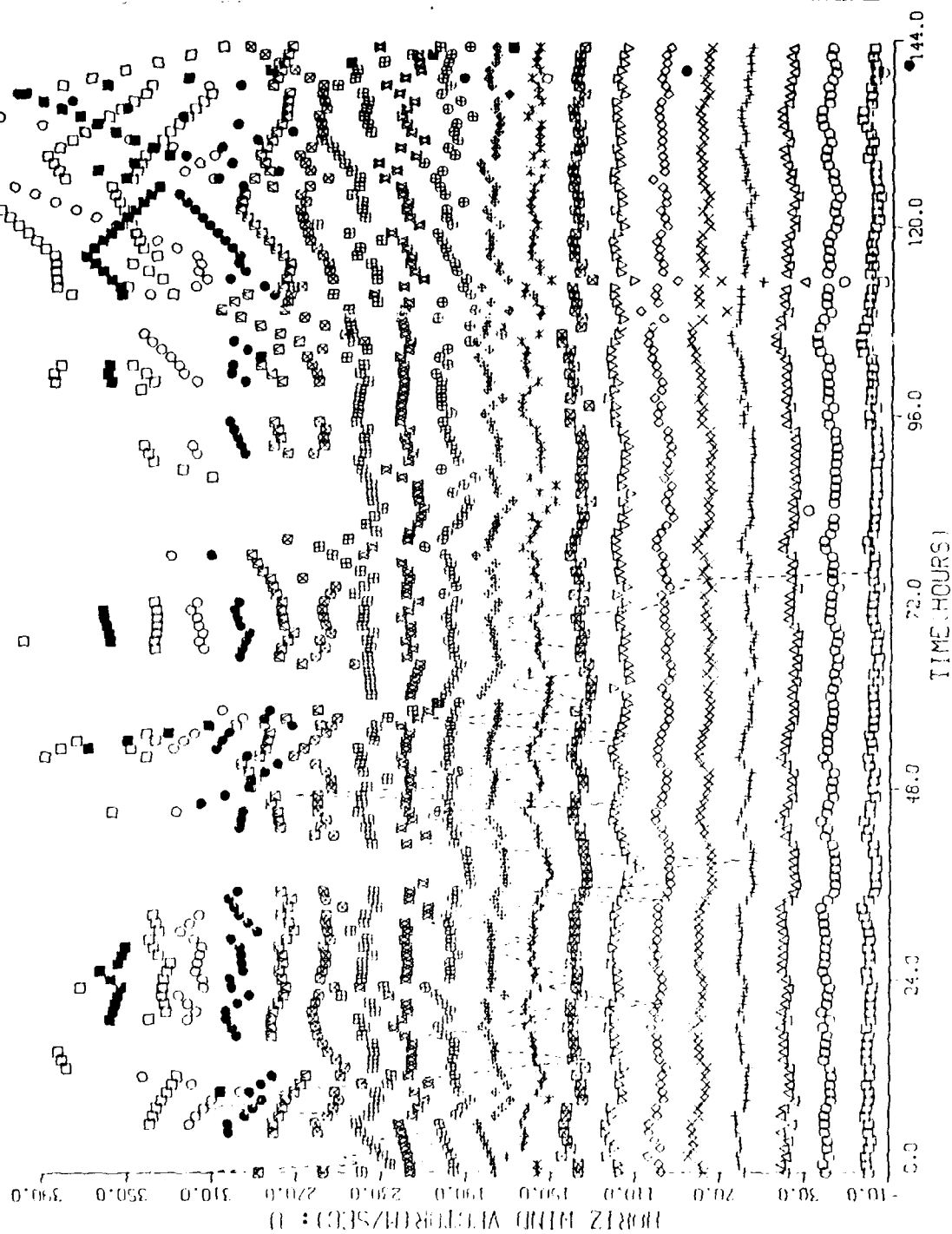


Figure 8. Horizontal Wind Vector (M/Sec): U

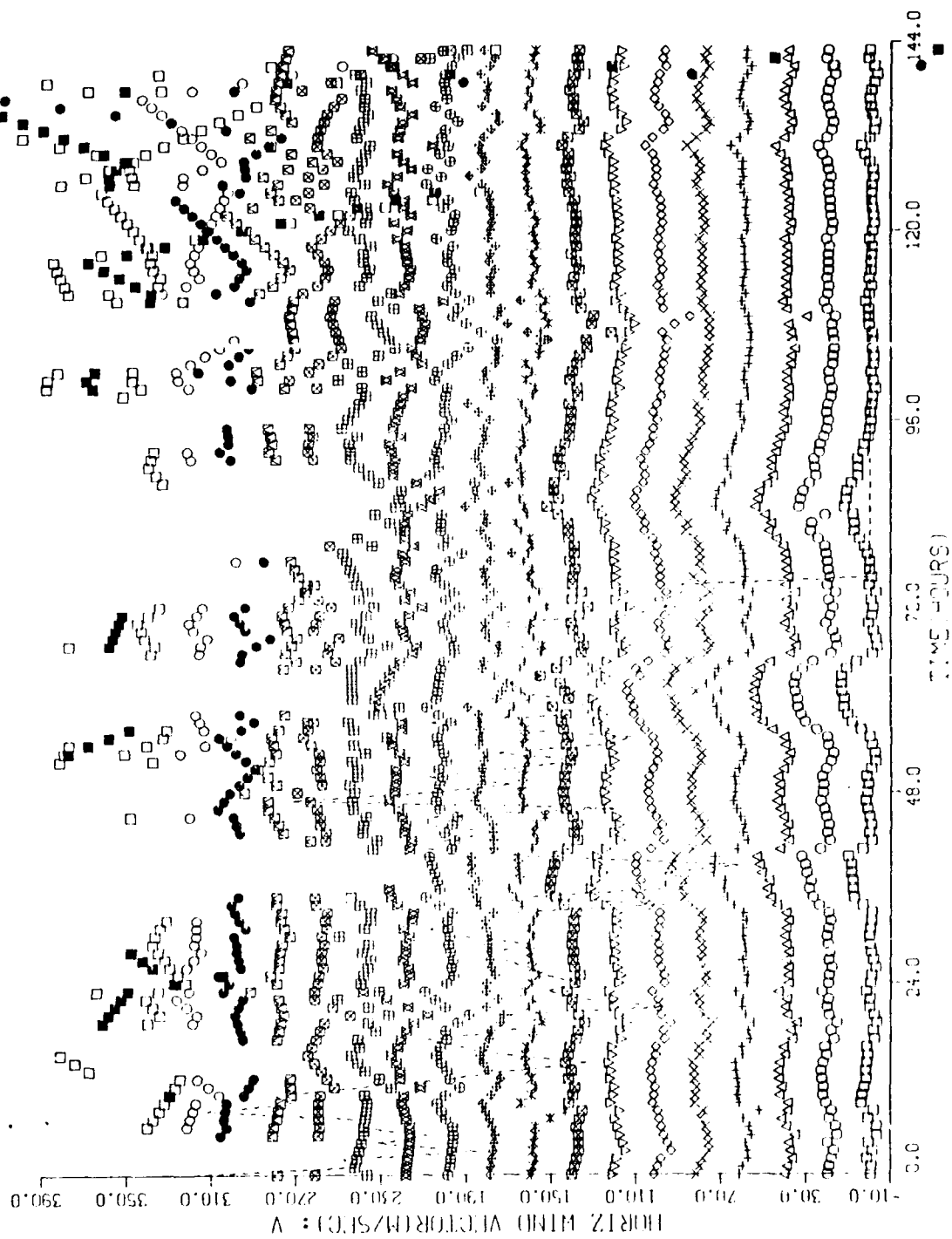


Figure 9. Horizontal Wind Vector (M/Sec): V

systems experience difficulty in measuring the wind structure above the inversion because of a loss of backscattered power due to the low turbulence level. Because of the loss of signal at the upper levels, only the lowest ten levels were processed in the spectral analysis.

E. SPECTRAL ANALYSIS OF THE DATA

All of the segments are of 64 (2^6) hours to accommodate the fast Fourier transform used in spectral analysis of the data. For analysis purposes, the 8 to 12 September 1985 data collection period is divided into two segments. Segment one covers hours 0 through 63 and segment two covers hours 57 through 120. Since the 8-12 September collection period is only 120 hours long, a seven-hour overlap of the two segments is necessary to keep the length of the segments fixed at 64 hours. The 21-29 September period is divided into segment one, which covers hours 0 through 63, segment two, which covers hours 64 through 127, and segment three, which covers hours 128 through 191. The 6-11 October period is divided into segment one, which covers hours 0 through 63, and segment two, which covers hours 64 through 127.

Since the fast Fourier transform method was used as part of the analysis, it was first necessary to detrend the data to avoid producing artificial discontinuities during analysis and to improve the statistical stability of the frequency contributions of wind variability (Bingham, et.

al., 1967 and Chatfield, 1984) Since the variation of the mean wind components was not linear over each Fourier transform period, a quadratic trend was calculated over each of the continuous segments in order to obtain mean u-component and v-component values. The perturbation u and v values were obtained by subtracting the mean values (trend) from the original values.

Two types of spectral analysis are used to study the variability of the u and v components. A power density spectrum represents the distribution of variance of a variable over frequency (Chatfield, 1984). In our case, the variables of interest are the u and v wind components, where the kinetic energy of the wind fluctuations is proportional to the variance. A rotary spectrum is a representation in frequency space of the power density spectrum of a two-dimensional vector time series (O'Brien and Pillsbury, 1974). The asymmetry of the rotary spectrum about the zero frequency may be used to infer rotational characteristics of the wind vector at various frequencies. The degree of asymmetry about the zero frequency indicates the degree of vector rotation. If the rotary spectrum has a peak at a positive frequency and a zero amplitude as the corresponding negative frequency, then pure clockwise rotation exists at that frequency. Conversely, there is pure counterclockwise rotation associated with a similar peak at a negative

frequency. If both the negative and positive frequency peaks have equal amplitudes, then there is no net rotation and instead there is pure oscillation. The sign of frequency that can be assigned to the clockwise or counterclockwise vector rotation is arbitrary. The convention chosen for this thesis is such that if the rotation is viewed with the u-component increasing towards the right and the v-component increasing upwards, then clockwise rotation corresponds to spectral peaks of positive frequencies and counter-clockwise rotation corresponds to spectral peaks of negative frequencies.

This thesis intends to interpret power density spectra and rotary spectra analyses to explore the vertical structure of the wind in the ABL in the Santa Barbara Channel. By using spectral analysis in tandem with inspection of the time series of the data, this thesis seeks to determine dominant regimes in the wind structure, the strength and frequency of sea and land breezes, the effect of synoptic-scale weather features on sea and land breezes, the influence of mesoscale cyclonic circulations, and the influence of topography near the sodar and rotation of the wind in the vertical.

III. PRESENTATION OF RESULTS

A. EVALUATION OF THE LOW-LEVEL WIND FIELD DURING SCCAMP

Synoptic-scale surface analyses indicate that the winds in and around the channel are normally westerly at 10 knots or less. The sodar data did not agree well with the synoptic data. This was especially true during the afternoon, when the sodar indicated an overwhelming northward wind component. At the same time, the synoptic data consistently showed eastward winds in the Santa Barbara Channel. At other times of the day, the synoptic winds were light and variable, which precluded any direct comparison with the sodar data. Also, the density of the synoptic data in the vicinity of the Santa Barbara Channel is coarse when compared to a single sodar station, which makes direct comparisons between the synoptic data and the sodar data very difficult.

From 8-12 September 1985, the synoptic analyses indicate southern California was affected by high pressure ridging associated with the eastern Pacific subtropical anticyclone. National Weather Service synoptic surface analyses indicate that early on 9 September, the Santa Barbara Channel was affected by a cold frontal passage (Fig. 10). This frontal passage interrupted the persistent northwesterly flow from

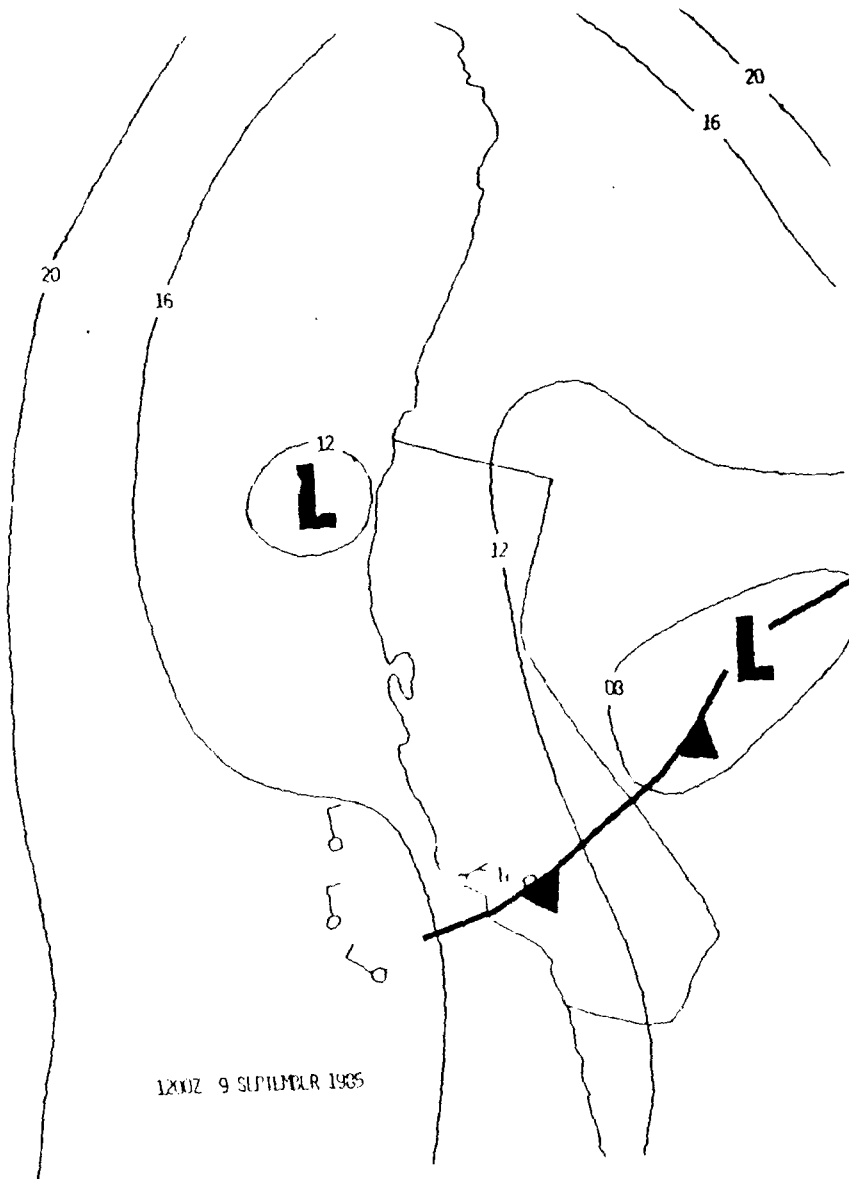


Figure 10. A Cold Frontal Passage over the Santa Barbara channel interrupts the synoptic northwesterly flow.

the eastern Pacific subtropical anticyclone. After the cold frontal passage, the persistent northwesterly winds off southern California returned. In segment one, the inversion height is relatively low and ranges from level 5 to level 9. During segment two, the inversion height varies between levels 10 and 20 (Fig. 4). During the 8-12 September period, each segment shows differing wind component patterns. Segment one shows eastward and northward components of 3 m/s in the morning and the resultant wind is northeastward. In the afternoon, there is a westward component of 2 to 5 m/s and a northward component of 7 to 8 m/s, and the resultant wind is north-northwestward. In the evening, there is a westward component of 2 to 4 m/s and a northward component of 1 to 2 m/s. The resultant wind is west-northwestward. Segment two during the morning indicates an eastward component of 4 to 5 m/s and a northward component of 0 to 2 m/s. The resultant wind is east-northeastward. During the afternoon, there is a westward component of 3 to 6 m/s and a northward component of 9 to 11 m/s (Fig. 11). The resultant wind is north-northwestward. In the evening, there is a westward component of 3 to 5 m/s and a southward component of 4 to 5 m/s, and the resultant wind is southwestward.

During 21-29 September the synoptic analyses (Fig. 12) indicate southern California was dominated by a thermal

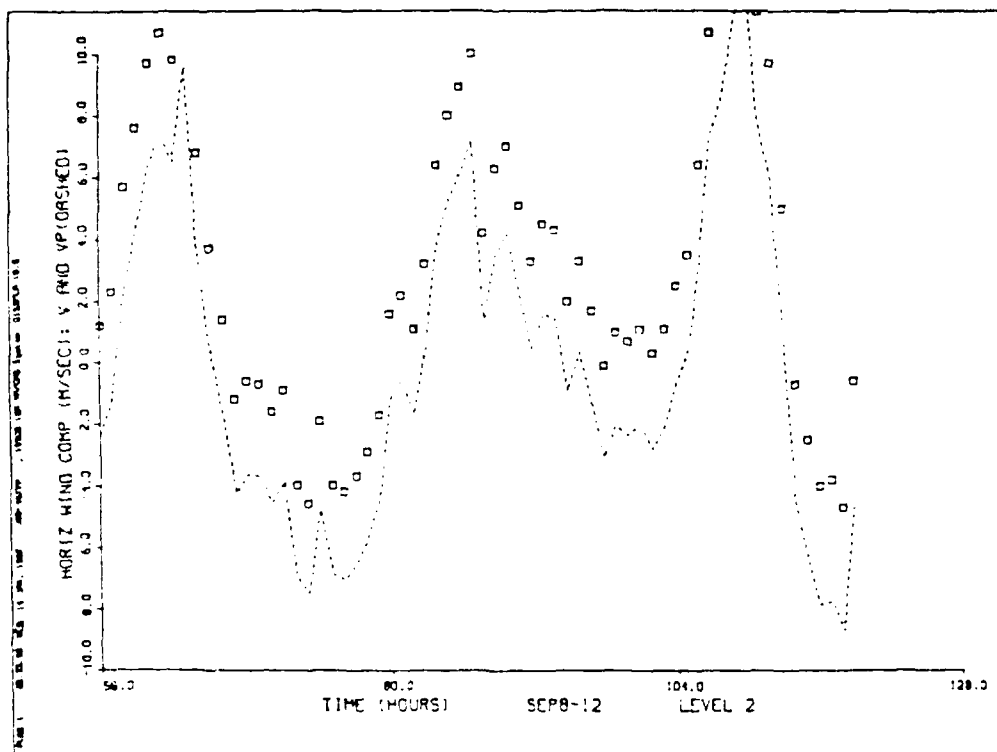


Figure 11. A Time Series of the v-component shows strong sea and land breezes occurring daily during 8-12 September 1985.

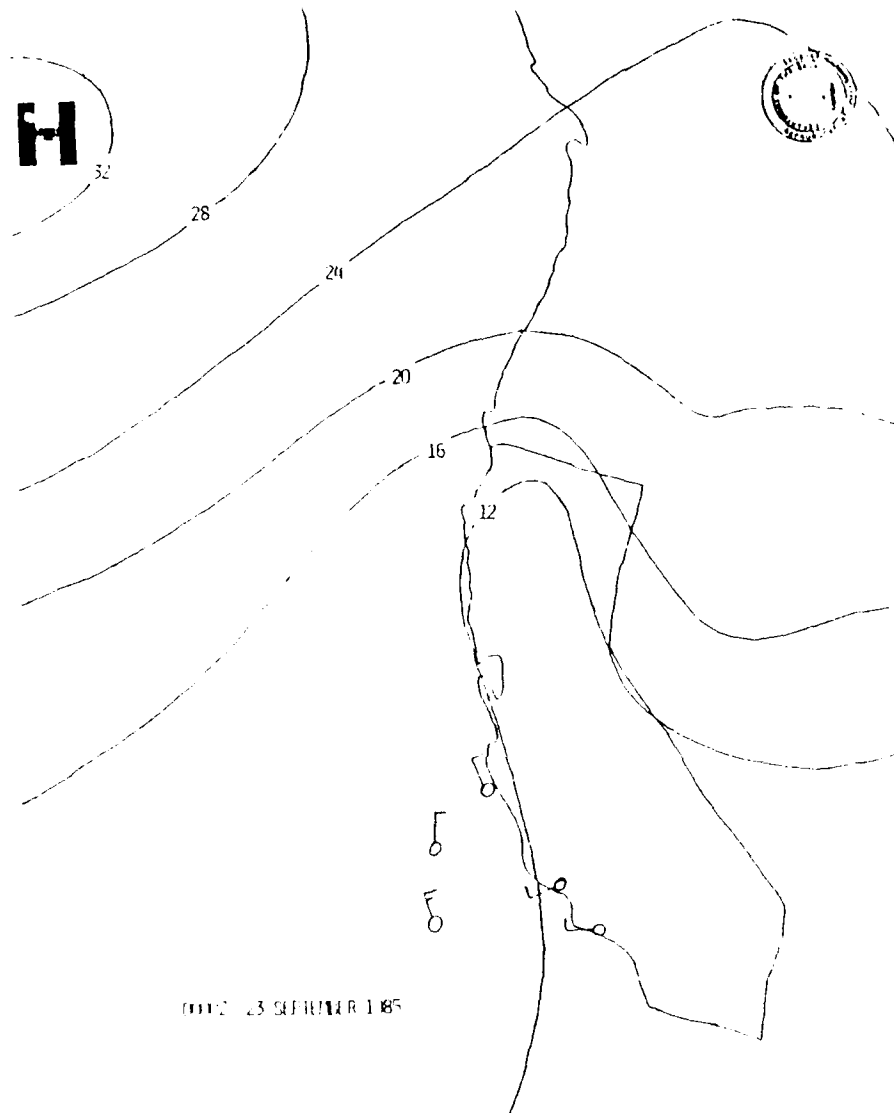


Figure 12. Southern California is dominated by a thermal trough and weak synoptic flow during 21-29 September.

trough, and weak synoptic flow. There were no frontal passages over southern California during this period. In segment one the inversion height is relatively high, ranging from levels 9 to 12. The inversion height lowers appreciably during segments two and three, when it ranges from levels 5 to 9 (Fig. 7). In the morning, segment one shows eastward (Fig. 13) and southward wind components of 3 to 6 m/sec, and the resultant wind is southeastward. During the afternoon, there is a westward component 2 to 4 m/sec and a northward component of 4 to 5 m/sec, which yield a northwestward resultant wind. In the evening there is a westward component of 1 to 2 m/sec and a southward component of 0 to 3 m/sec. The resultant wind is south-southwestward. Segment two indicates a morning eastward wind component of 2 to 6 m/sec and a southward component of 2 to 7 m/sec, with a resultant southeastward wind. During the afternoon, there is a westward component of 1 to 4 m/sec and a northward component of 2 to 4 m/sec, which produces a resultant northwestward wind. In the evening, there are eastward and westward components of 1 to 2 m/sec, and a southward component of 4 to 6 m/sec. The resultant wind is south-southwestward. Segment three shows an eastward component of 2 to 6 m/sec, plus southward and northward components of 2 to 3 m/sec during the morning. The resultant wind is eastward. In the afternoon there is a westward component of

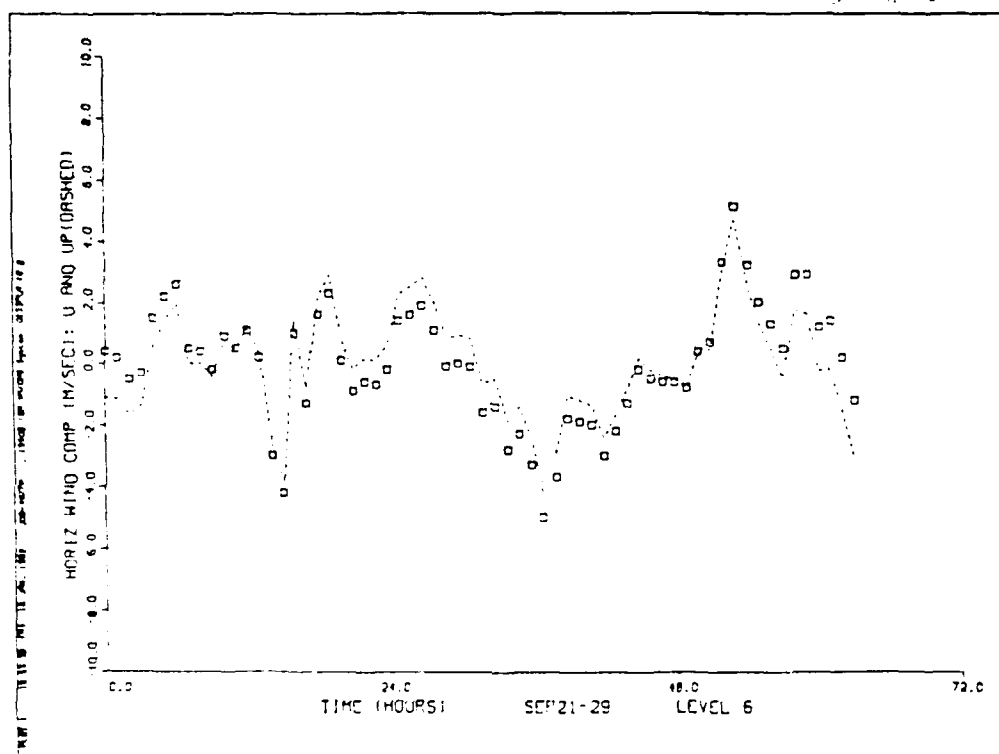


Figure 13. A Time Series of the u-component indicates positive, -u or eastward wing components, during the morning period.

1 to 5 m/sec and a northward component of 4 to 5 m/sec, which yields a north-northwestward resultant wind. During the evening there is a westward component of 1 to 3 m/sec and a southward component of 2 to 3 m/sec. The resultant wind is southwestward.

From 6-11 October, synoptic analyses show that southern California is in a thermal trough, except during 8 October, when a cold front passed through the area (Fig. 14). During segment one, the inversion height is fairly low, ranging from levels 7 to 9 (Fig. 9). Inversion height data are not available for segment two. In segment one and during the morning, there is an eastward wind component of 3 to 5 m/sec and a southward component of 0 to 5 m/sec. The resultant wind is southeastward. During the afternoon there is a westward component of 3 to 6 m/sec and a northward component of 10 to 11 m/sec, which produces a resultant north-northwestward wind. In the evening, there is a westward component of 2 to 3 m/sec and a southward component of 3 to 4 m/sec, which yields a southwestward resultant wind. During segment two and in the morning, there is an eastward wind component of 3 to 5 m/sec and a southward component of 2 to 5 m/sec. During the afternoon, there is an westward component of 3 to 6 m/sec and a 10 to 11 m/sec northward component. The resultant wind is north-northwestward. In



Figure 14. A Second Cold Frontal Passage Affected the Santa Barbara Channel during 6-11 October.

the evening there are westward and southward components of 3 to 5 m/sec, producing a southwestward resultant wind. During the morning, resultant winds range from northeastward to south-southeastward and are being influenced by a persistent synoptically-driven eastward wind component in every segment. Afternoon resultant winds range from northwestward to north-northwestward. Apparently, the sea breeze is being deflected to the west. The cause of the westward wind component in all seven segments is not known. In the evening, resultant winds range from south-southwestward to southwestward, with the exception of one segment, when the resultant wind is west-northwestward. It appears that the land breeze is being deflected westward by Coriolis force. The sea breezes are twice as intense during periods that experienced cold frontal passages (7-11 m/sec), compared to the period when there were no frontal passages (2-5 m/sec). The v-component was much stronger during 8-12 September and 6-11 October and much weaker during 21-29 September. The observations concerning the sea breeze (northward flow) and land breeze (southward flow) in the Santa Barbara Channel region agree fairly closely with those made by Caldwell, who used data from the OPUS II experiment. After being interrupted by a cold frontal passage, the synoptic northwesterly flow once again begins to re-establish itself. At the beginning of a northwesterly wind

event, or after a frontal passage, the sea breeze becomes strong (Caldwell, et. al., 1986). As the northwesterlies re-establish and strengthen, they create synoptic-scale subsidence and clear skies, allowing for increased solar heating of the land during the daytime, which initiates a sea breeze circulation (Caldwell, et. al., 1986).

The northward wind components of about 11 meters per second that occurred after the 9 September and 8 October frontal passages are large values for a pure sea breeze. Southward wind components ranging from 4 to 6 meters per second that occurred during all three periods may be considered to be significantly large values for a pure land breeze. Data on the land breeze are scarce, although definite surges of the land breeze of up to 5 meters per second have been observed in the tropics (Atkinson, 1981). The cold frontal passages affecting the Santa Barbara Channel during the SCCAMP experiment were relatively weak, with a temperature contrast of 3 to 4 degrees Fahrenheit. Thus, it is quite possible that the large values noted for the northward and southward wind components were not caused solely by sea and land breezes, but by sea and land breezes enhanced by upslope and downslope winds, respectively.

There are three persistent features in the wind structure during all of the segments. In the morning, an eastward wind component exists nearly every day in all ten

of the lower levels (Figs. 4, 6, 8 and 13). During the afternoon, a northward wind component is evident each day in all ten levels (Figs. 5, 7 and 9). In the evening, a southward wind component is present in almost all ten of the lower levels every day during the 8-12 September and 6-11 October periods (Figs. 5 and 9). The evening southward wind component is also evident on a daily basis during the 21-29 September period, but is not always present in the lowest three levels (Fig. 7). National Weather Service surface analyses (Fig. 14) indicate that the persistent northwesterly flow off the coast of southern California was interrupted by a second cold frontal passage on 8 October. Note how much more pronounced the northward and southward wind components become on the day before, during and after the frontal passage occurred (Fig. 9). This observation differs from results by Caldwell et. al. (1986), which indicate that the sea and land breezes do not intensify until the day after a cold frontal passage.

B. POWER DENSITY SPECTRA OF THE U-COMPONENT

For the 8-12 September period, there are similar energy distributions for segment one and segment two. Both segments show a dominant peak at the one cycle per day frequency in all levels, with the largest sub-diurnal peak at two cycles per day in the lower five levels (Figs. 15 and 16). This pattern exists at almost every level. The main

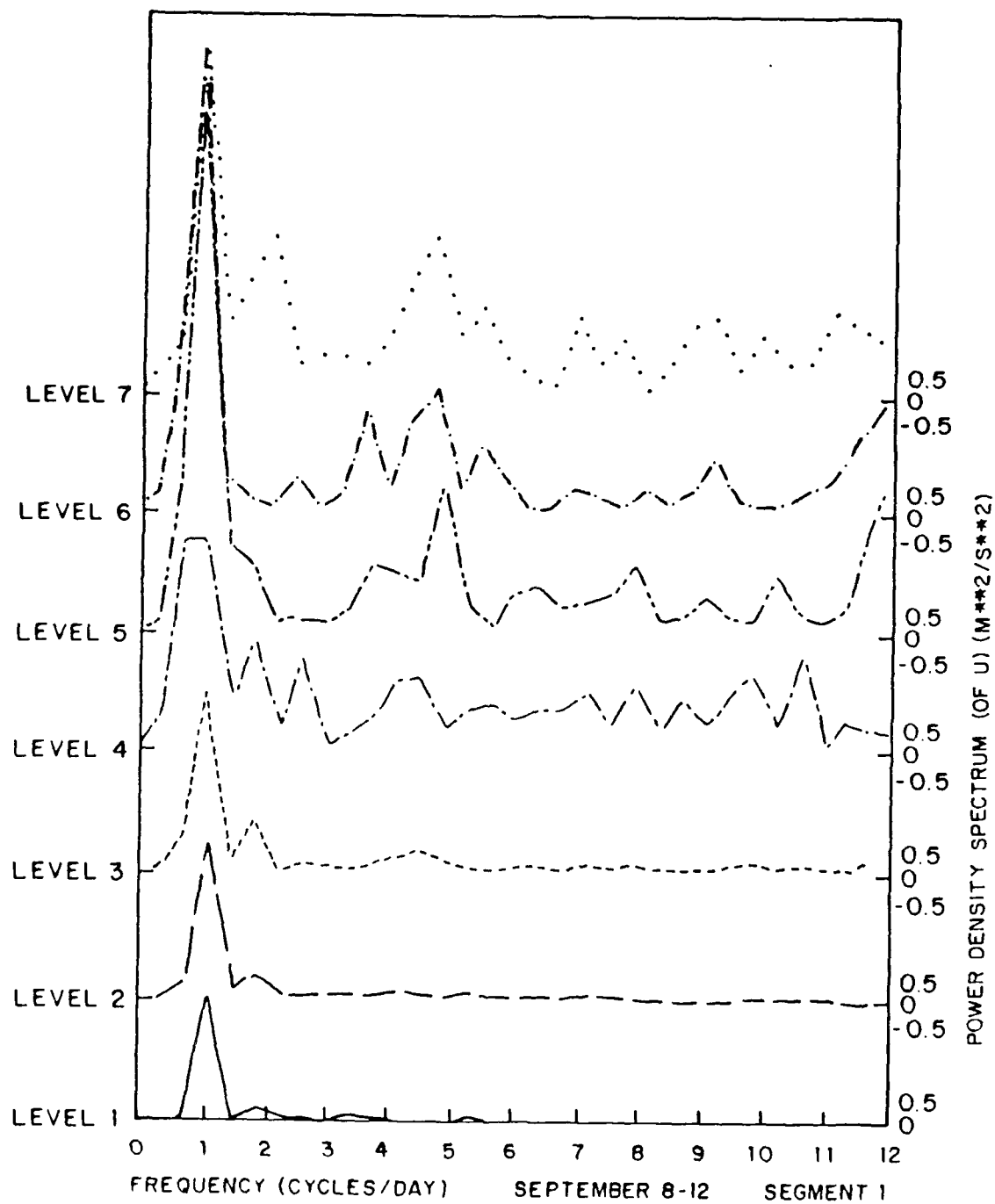


Figure 15. Power Density Spectrum (of U) (M^2/S^2)
September 8-12, 1985, Segment 1

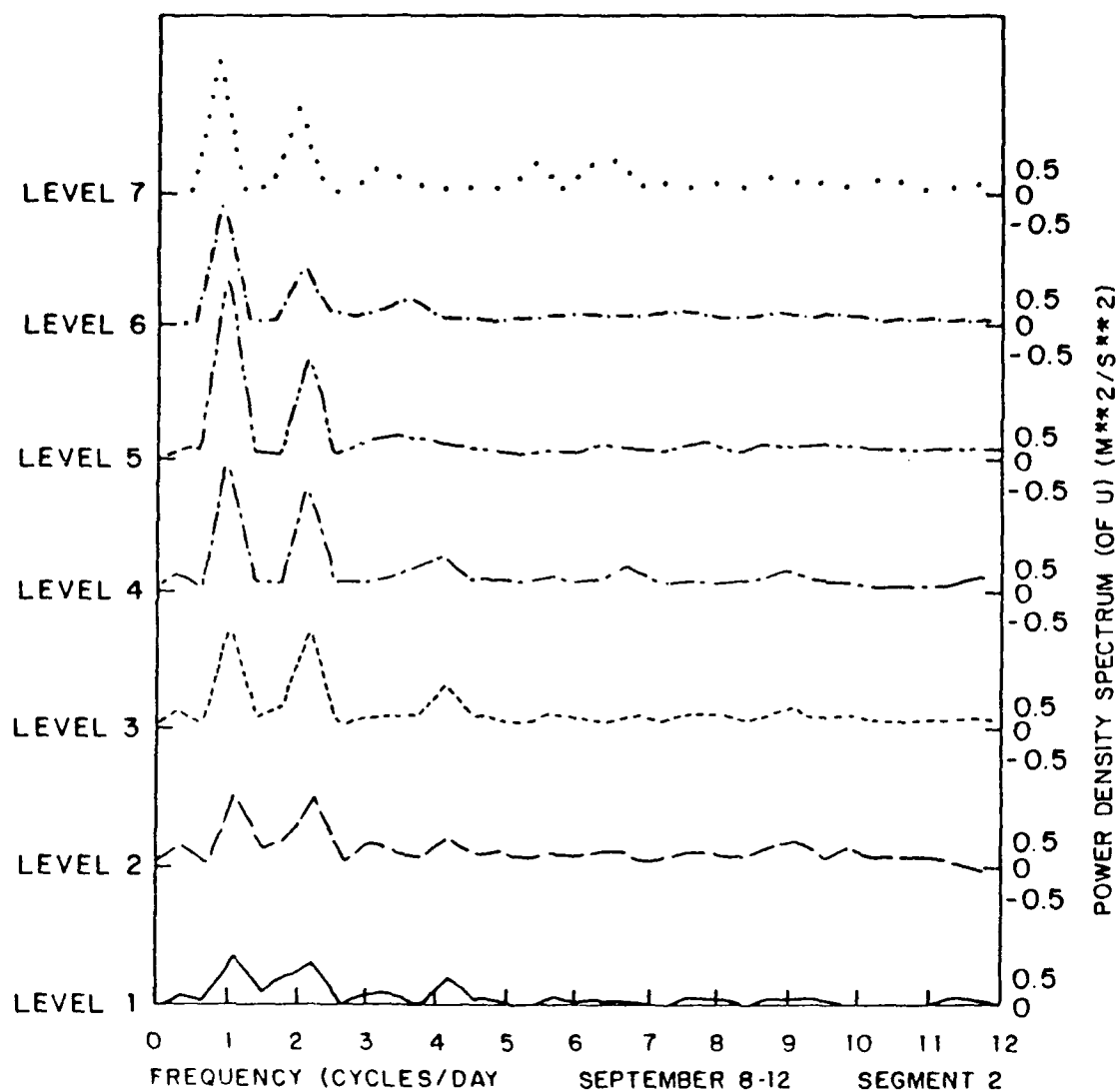


Figure 16. Power Density Spectrum (of U) (M^2/S^2)
September 8-12, 1985, Segment 2

difference between the two segments is that there is considerably more energy in segment one, as indicated by its stronger power density spectra peaks at one cycle per day (Fig. 15).

During 21-29 September 1985, the dominant peak in all three segments is at the diurnal frequency of one cycle per day in all levels (Figs. 17, 18 and 19). However, there is no dominant sub-diurnal peak at any frequency in any of the segments.

In segment one of the 6-11 October period, the dominant peak appears at two cycles per day in all levels, with a secondary peak at one cycle per day in almost every level (Fig. 20). Segment two indicates dominant peaks near one cycle per day in all levels, and a secondary peak at two cycles per day in the lower six levels, which progressively weakens with height (Fig. 21).

The dominant peak at the one cycle per day frequency in six of the seven segments and in all levels suggests that most of the energy in the ABL is related to the diurnal sea and land breeze cycles. This agrees with results from Caldwell, et. al. (1986), which state that diurnal influences are a dominant energy source in the Santa Barbara Channel. Dabberdt (1984) mentions that the Gaviota Eddy, a mesoscale circulation, often forms in the Santa Barbara Channel (Fig. 2). Wakimoto (1987) discusses the Catalina

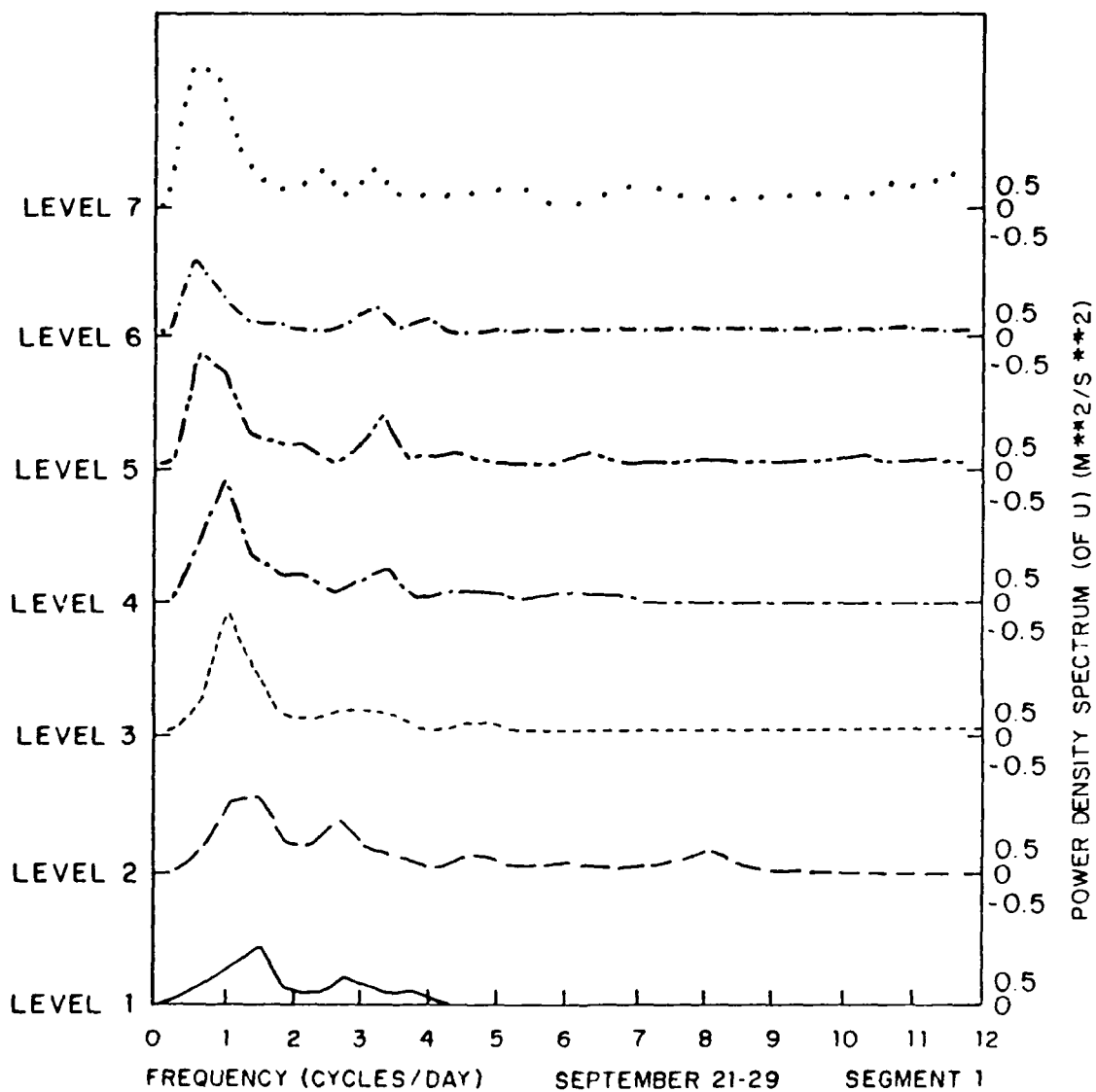


Figure 17. Power Density Spectrum (of U) (M^2/S^2)
September 21-29, 1985, Segment 1

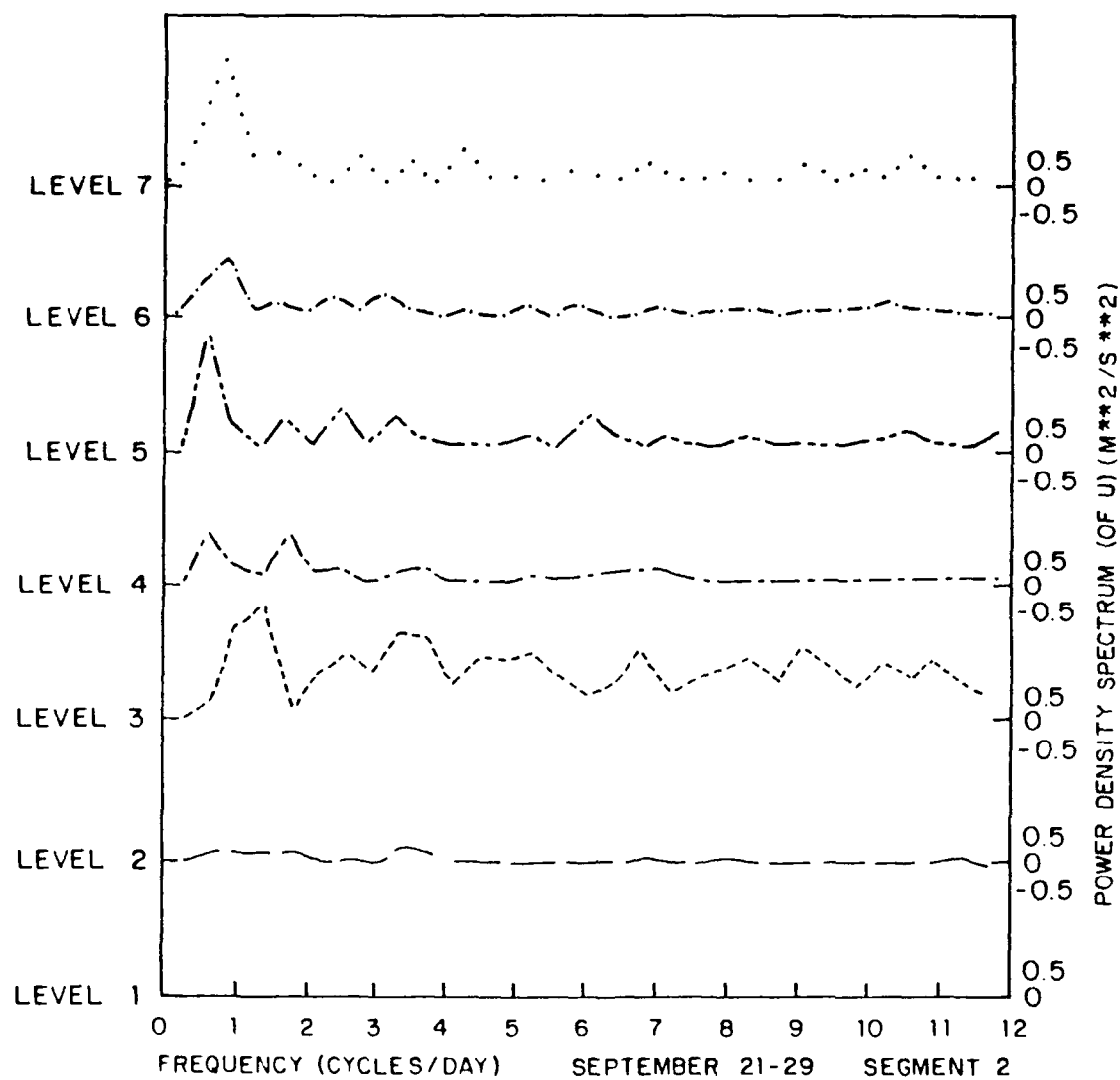


Figure 18. Power Density Spectrum (of U) (M^2/S^2)
September 21-29, 1985, Segment 2

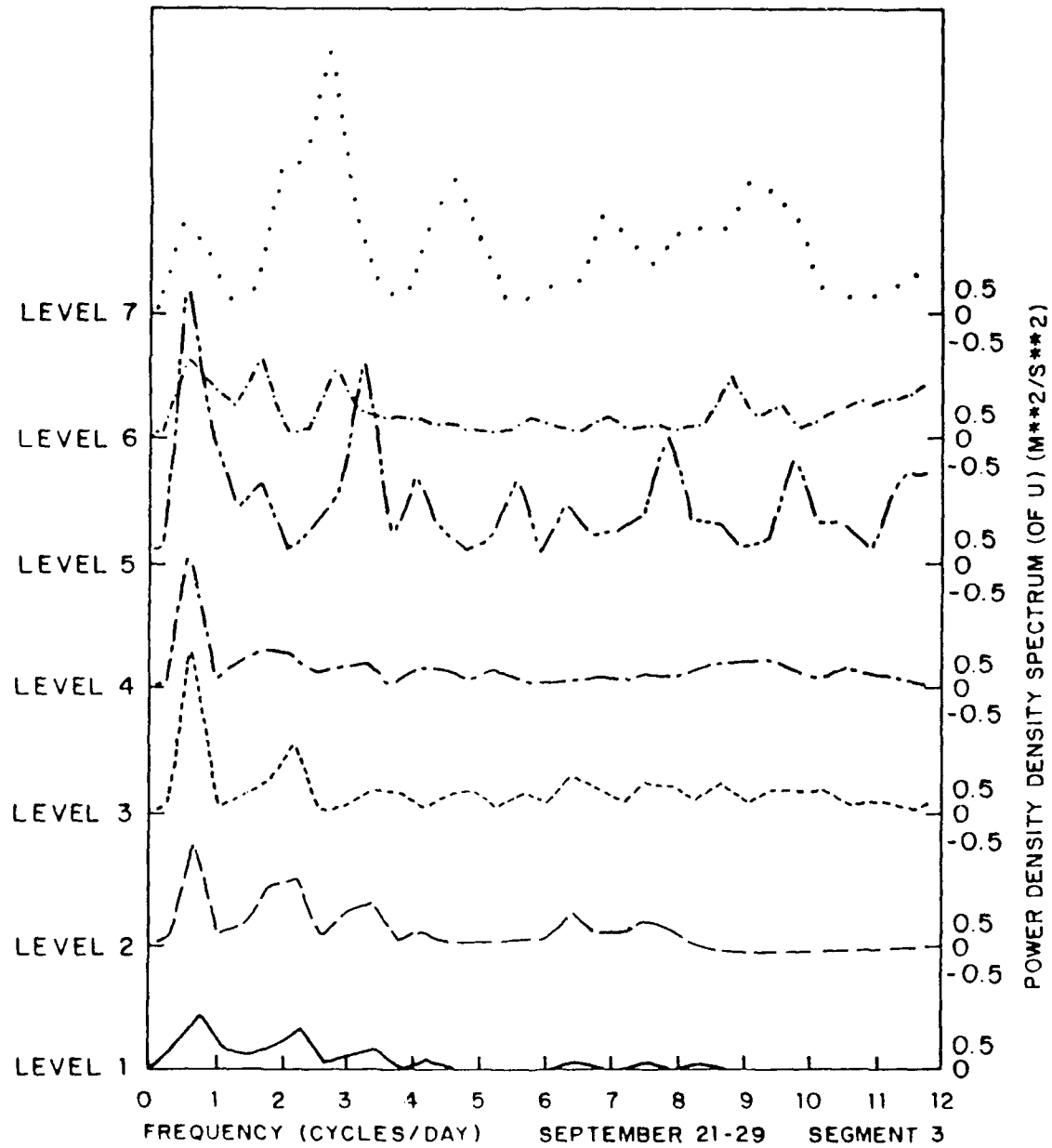


Figure 19. Power Density Spectrum (of U) (M^2/S^2)
September 21-29 1985, Segment 3

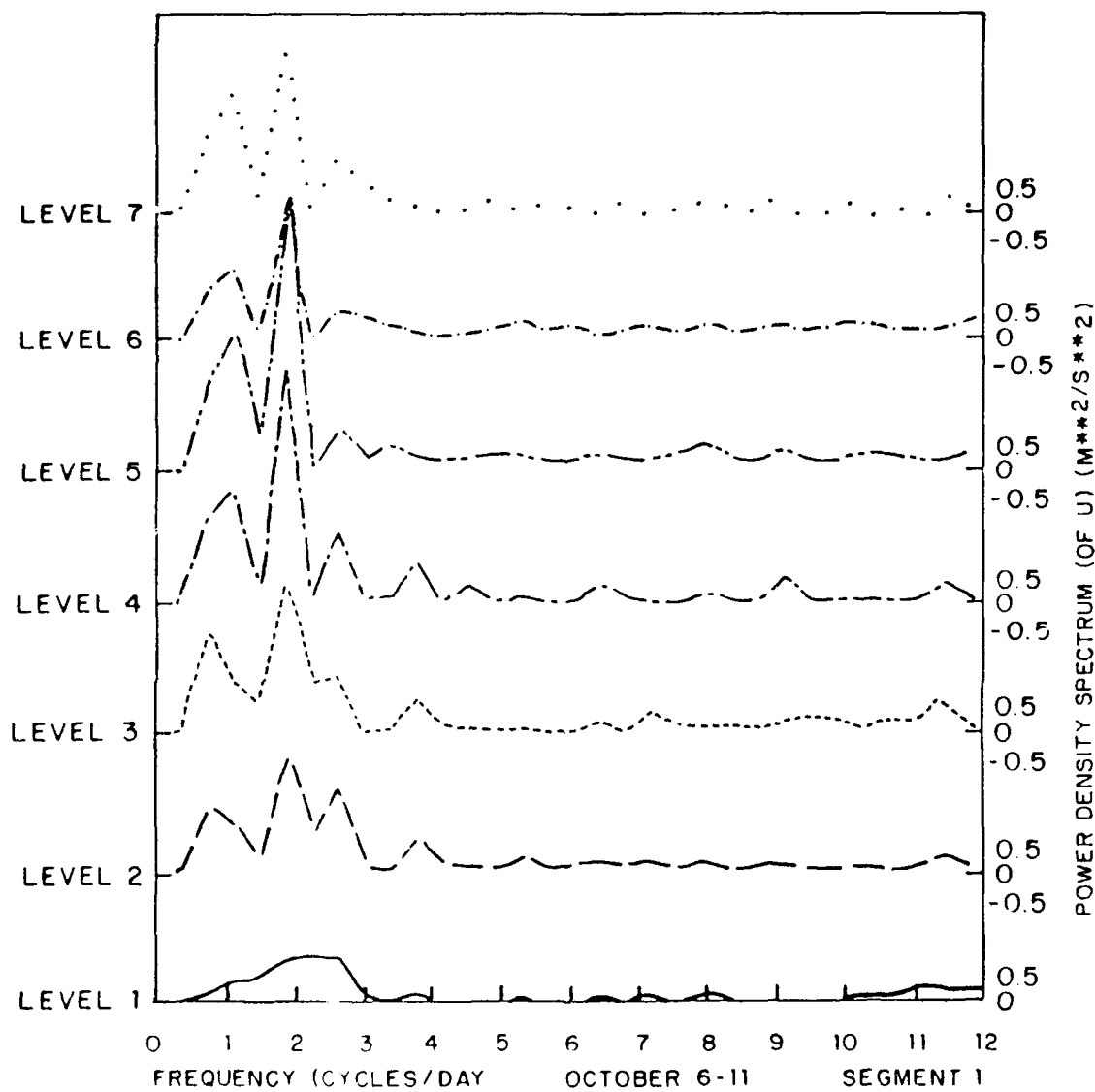


Figure 20. Power Density Spectrum (of U) (M^2/S^2)
October 6-11 1985, Segment 1

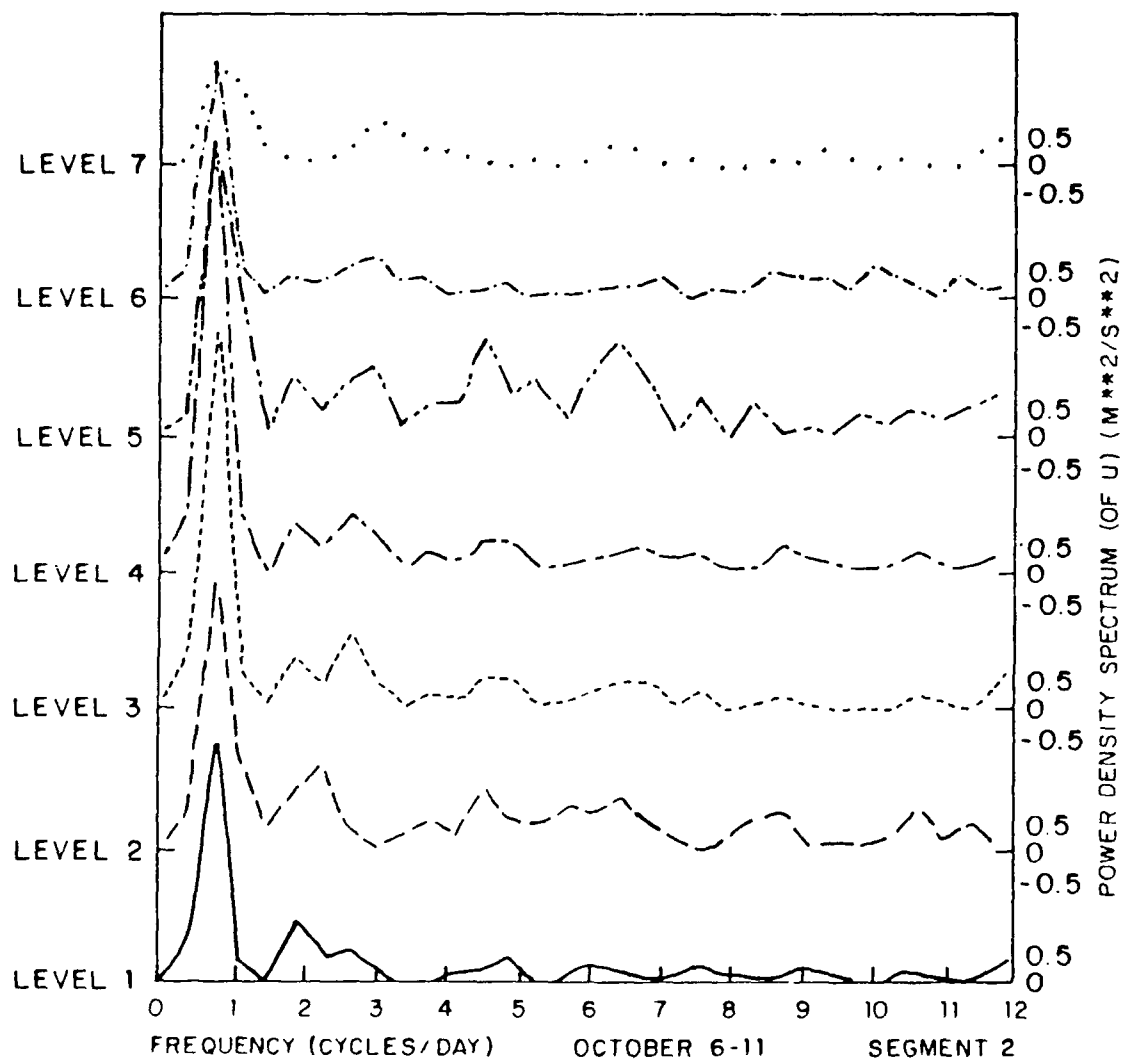


Figure 21. Power Density Spectrum (of U) (M^2/S^2)
October 6-11 1985, Segment 2

Eddy, which extends into the Santa Barbara Channel (Fig. 22). The shifting of these eddies with time in the Santa Barbara Channel may be related to the prevalent sub-diurnal frequency peaks observed at two cycles per day.

C. POWER DENSITY SPECTRA OF THE V-COMPONENT

During 8-12 September 1985, segment one shows a strong peak at one cycle per day that increases significantly with height in all levels (Fig. 23). There is a secondary peak which varies slightly in frequency from 2 to 2.5 cycles per day and intensifies with height in all levels. In segment two, there is an extremely large peak near the one cycle per day frequency, which may be related to the 9 September cold frontal passage (Fig. 24). There is also a secondary peak between the zero and one cycle per day frequencies, but it is extremely small in amplitude compared to the one cycle per day peak and is apparently due to noise in the data. From 21-29 September, two patterns are evident. In segment one, the one cycle per day peak intensifies with height and no prevalent sub-diurnal peak is present (Fig. 25). Segments two and three show a pattern opposite to that of segment one (Figs. 26 and 27). The one cycle per day peak weakens with height as a two cycle per day peak intensifies with height. For the 6-11 October period, each segment has its own energy distribution pattern. The one cycle per day peak weakens with height as the two cycle per day peak

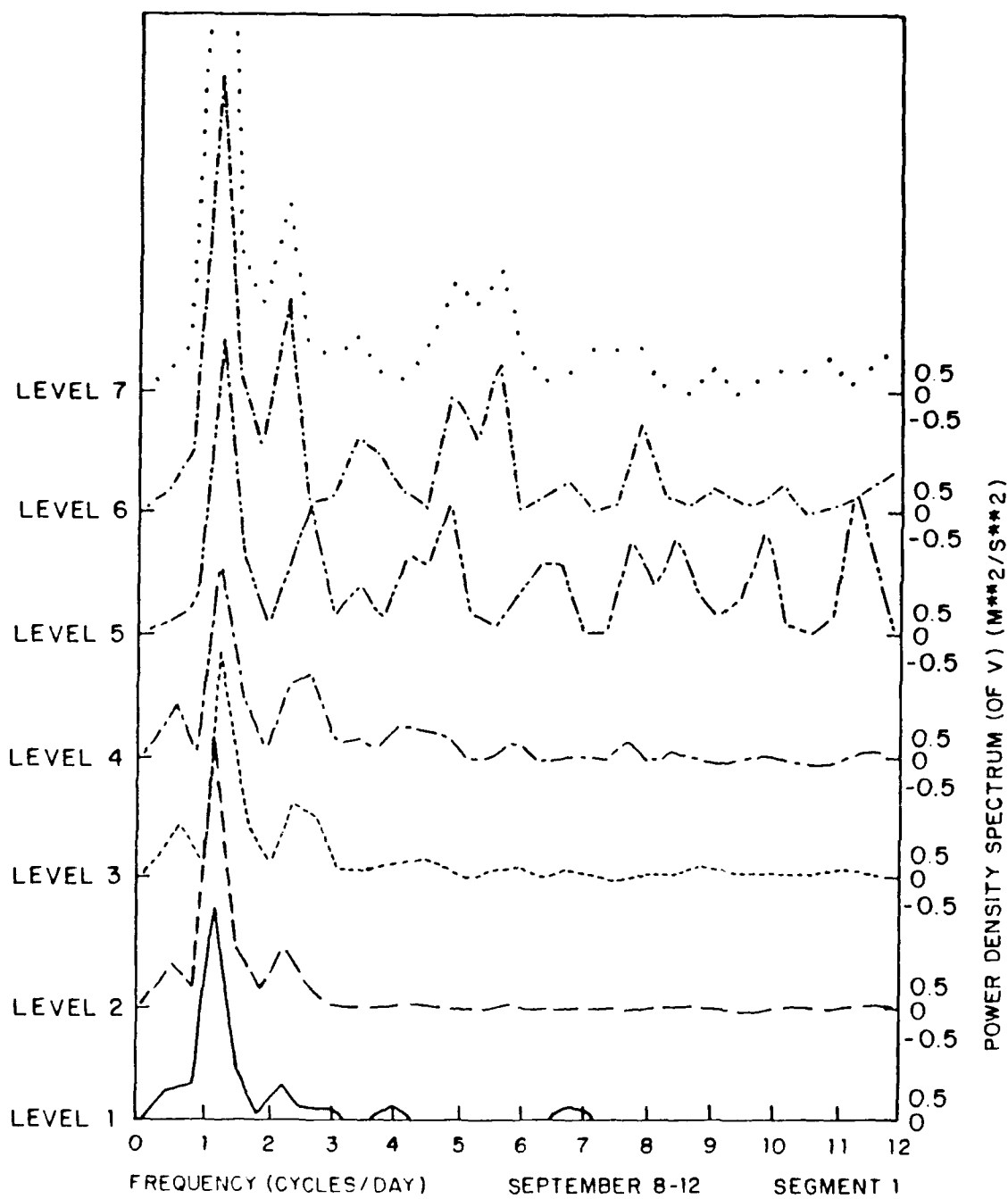


Figure 23. Power Density Spectrum (of V) (M^2/S^2)
September 8-12, 1985, Segment 1

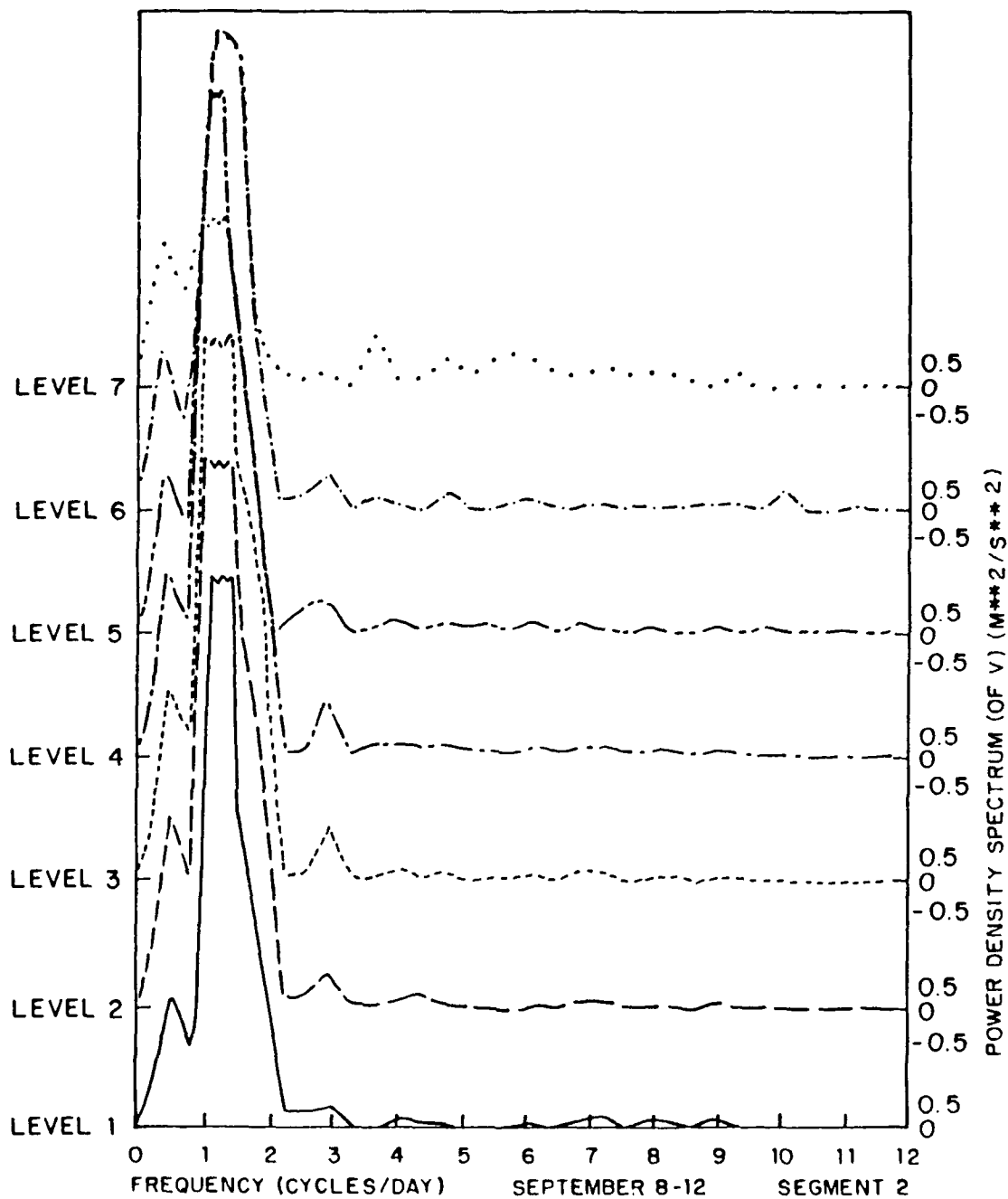


Figure 24. Power Density Spectrum (of V) (M^2/S^2)
September 8-12, 1985, Segment 2

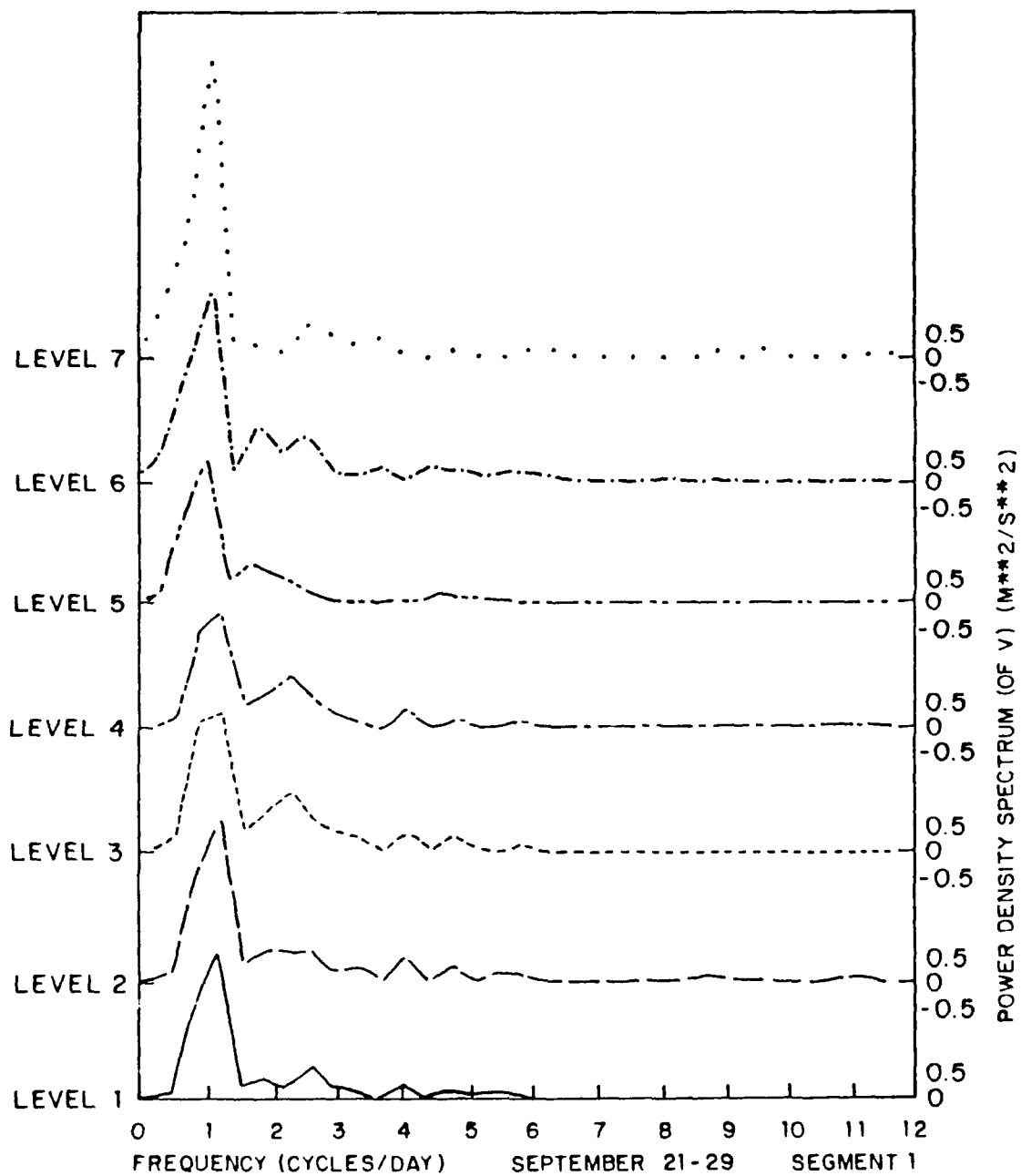


Figure 25. Power Density Spectrum (of V) (M^2/S^2)
September 21-29 1985, Segment 1

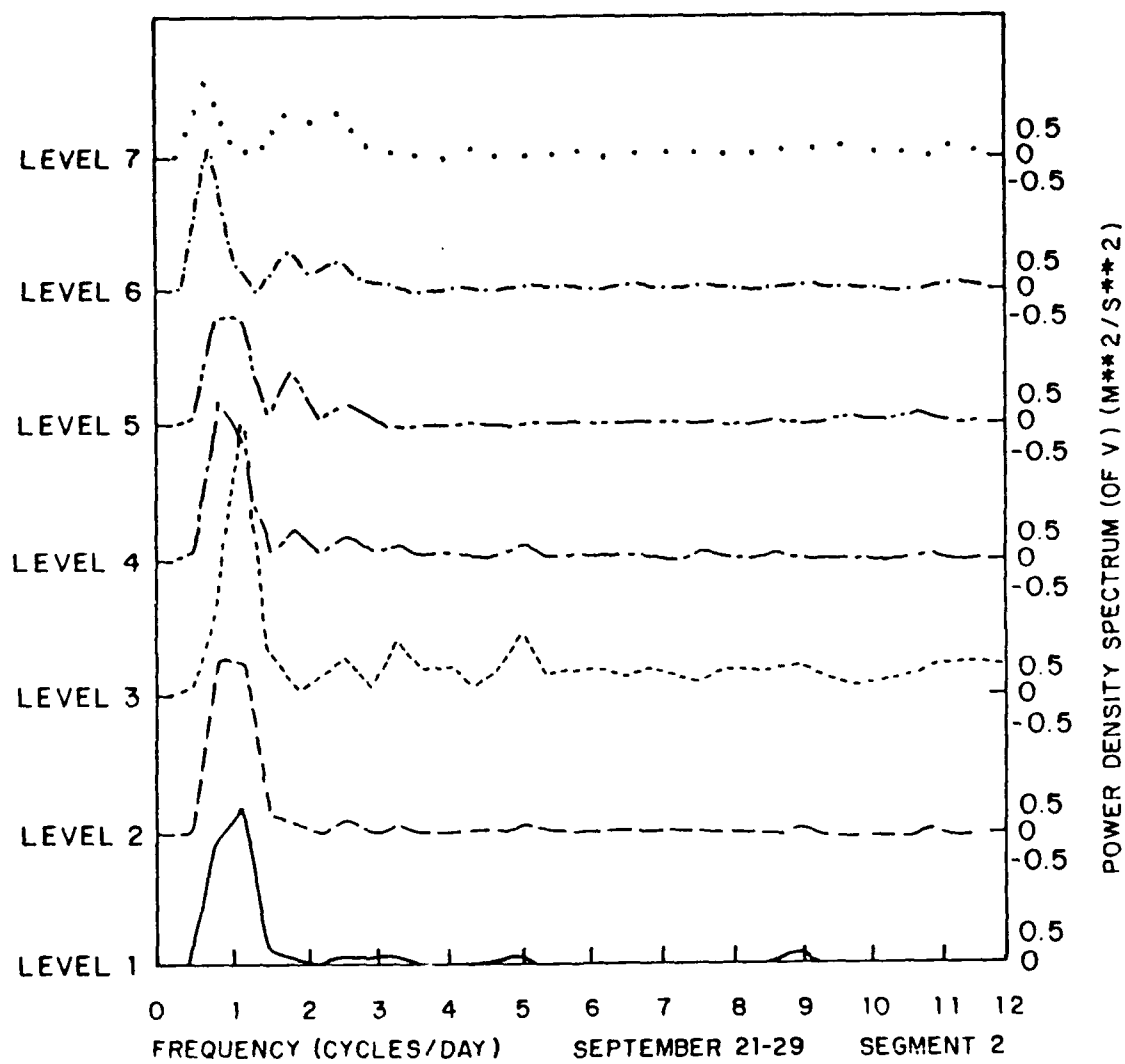


Figure 26. Power Density Spectrum (of V) (M^2/S^2)
September 21-29 1985, Segment 2

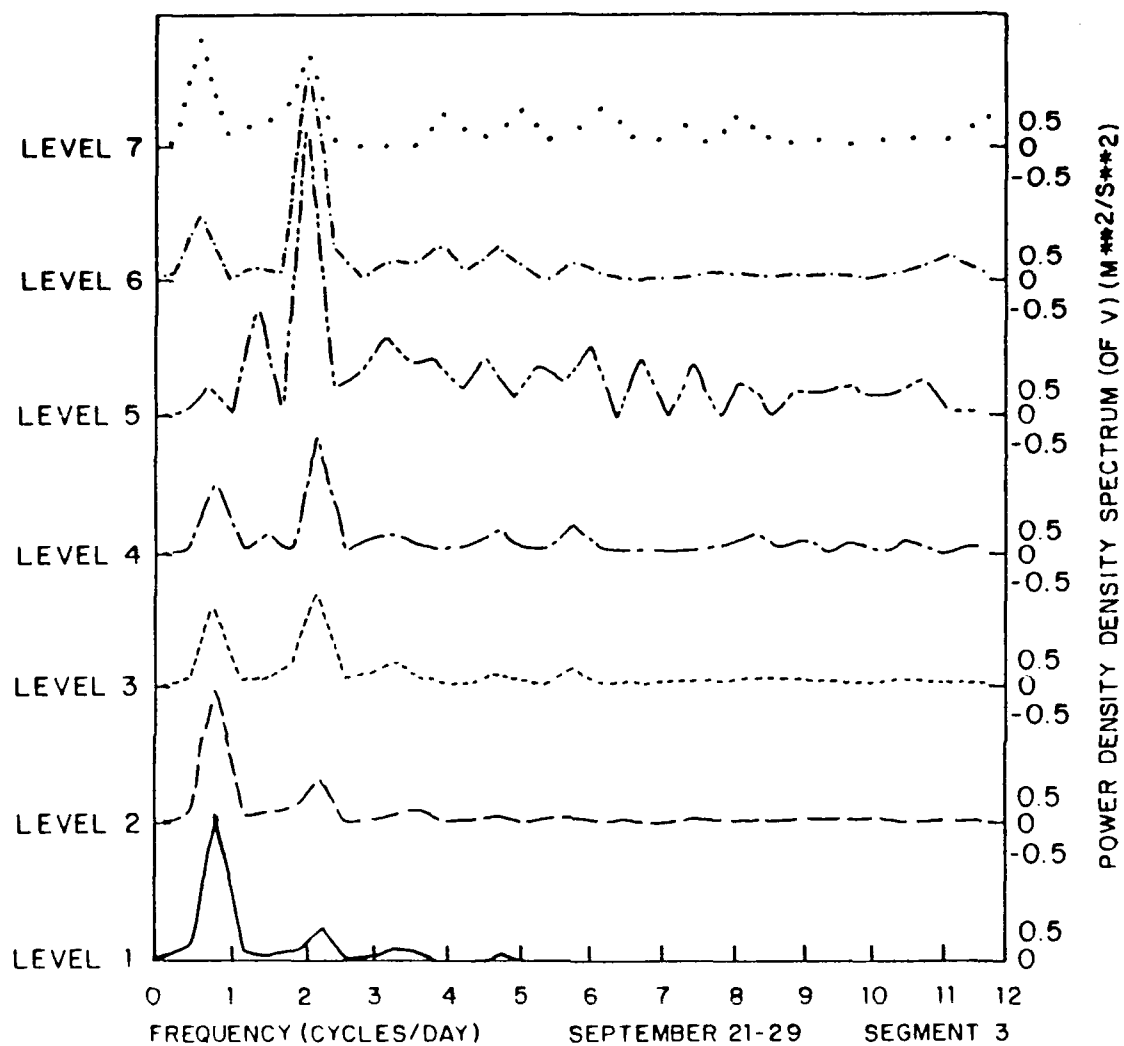


Figure 27. Power Density Spectrum (of V) (M^2/S^2)
September 21-29 1985, Segment 3

intensifies with height (Fig. 28). During segment two an extremely large peak dominates at one cycle per day in all levels, with a secondary peak at two cycles per day (Fig. 29). As is true for the power density spectra analysis of the u-component, the dominant peak in most of the segments exists at the one cycle per day frequency, which reinforces the suggestion made in the previous section that the diurnal sea and land breezes contribute most of the energy found in the Santa Barbara Channel's ABL. As is seen for the u-component, the power density spectral analysis of the v-component also shows a prevalent sub-diurnal peak near the two cycles per day frequency, and again could be related to a mesoscale eddy, as was suggested in the previous section. There is significantly more energy in the v-component than in the u-component. The power density spectra peaks at the one cycle per day frequency for the v-component are much larger than their counterparts for the u-component, which reflects the fact that the dominant energy is in the diurnal sea and land breezes. Another interesting result is that there is much more energy in the v-component during the 8-12 September and 6-11 October periods, when cold frontal passages affected the Santa Barbara Channel. During the 21-29 September period there were no frontal passages and the v-component spectral analysis indicates relatively small peaks at the one cycle per day frequency. This agrees with

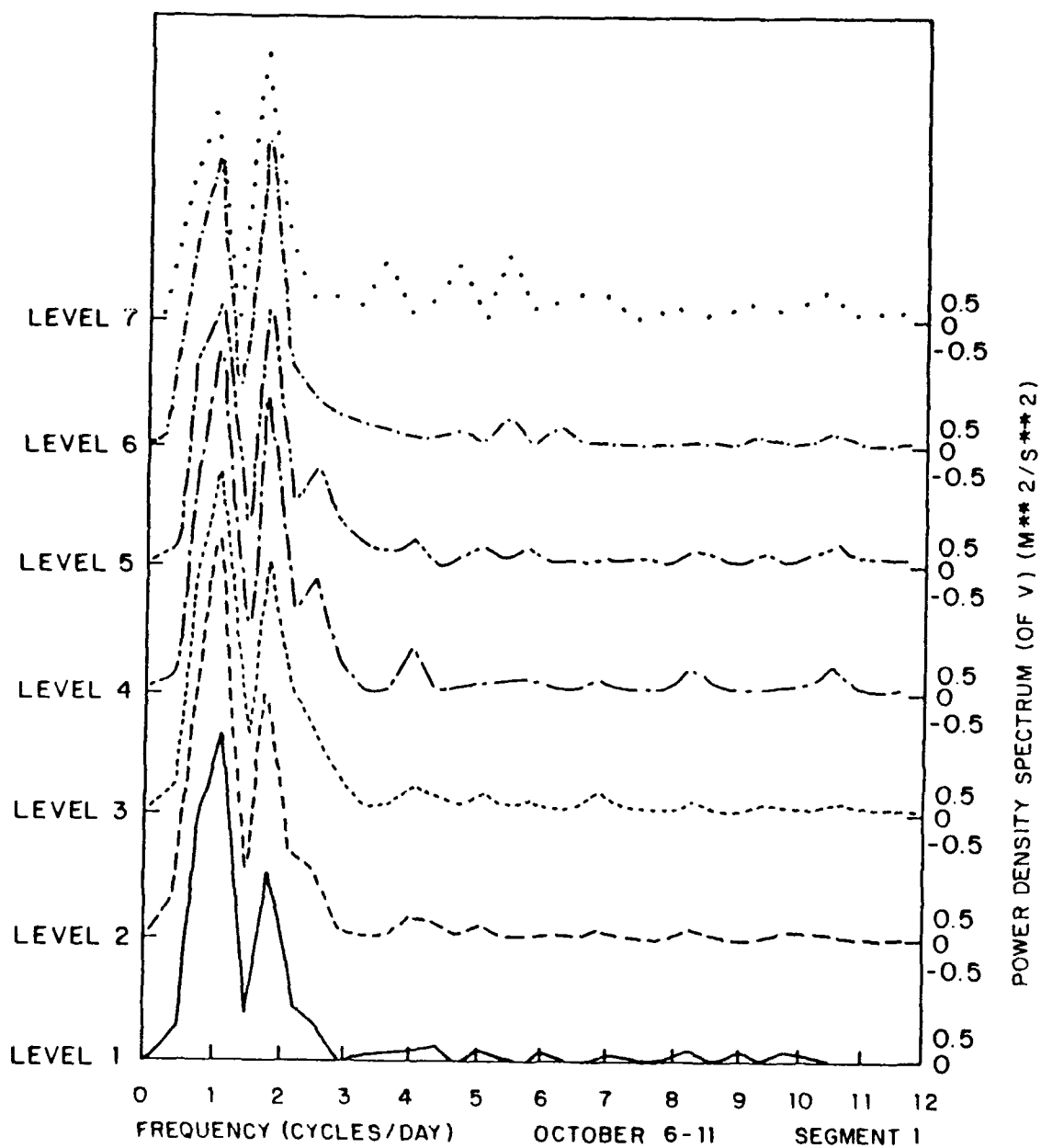


Figure 28. Power Density Spectrum (of V) (M^2/S^2)
October 6-11 1985, Segment 1

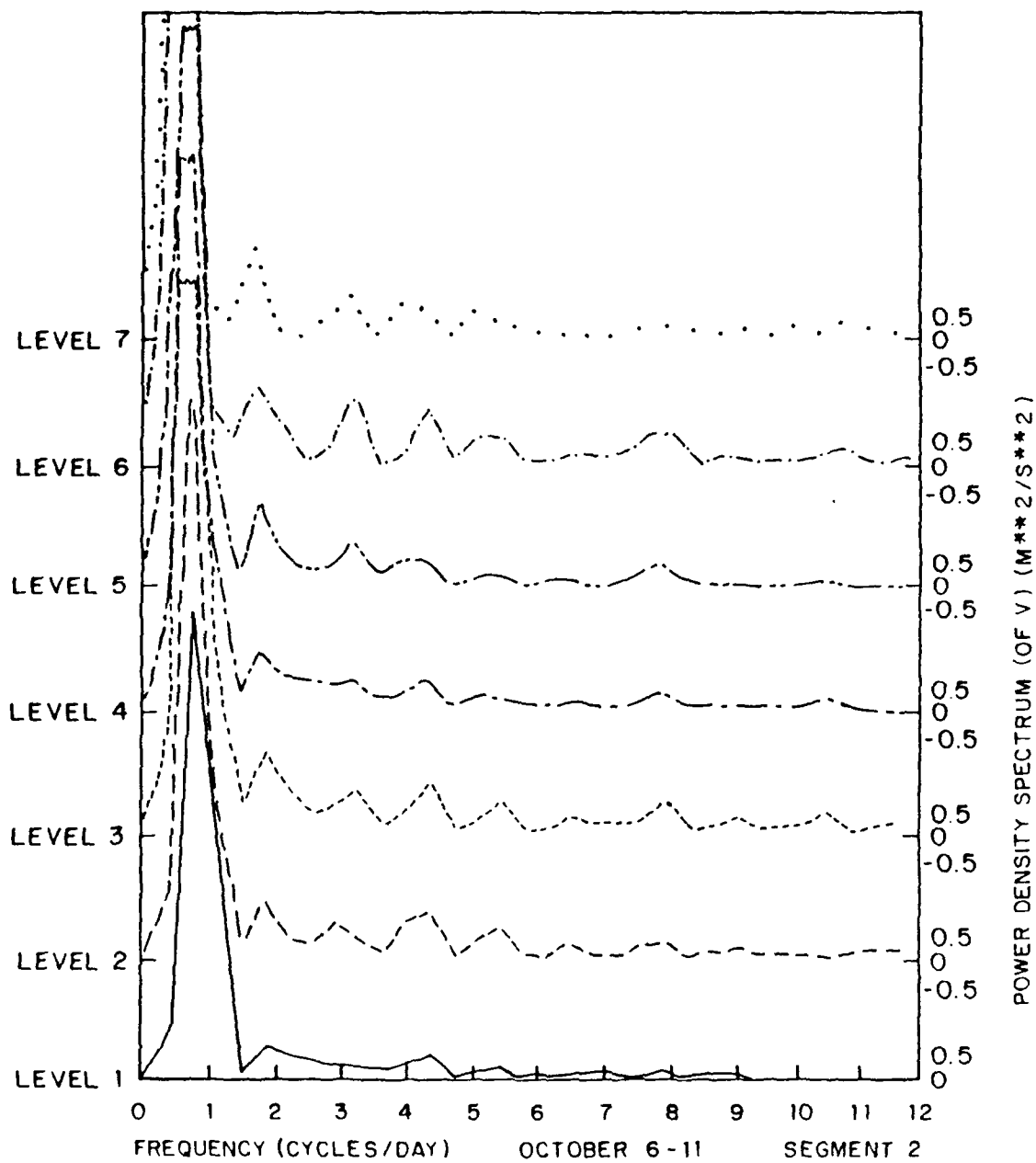


Figure 29. Power Density Spectrum (of V) (M^2/S^2)
October 6-11 1985, Segment 2

Caldwell, et. al. (1986), who state that cold frontal passages in the Santa Barbara Channel can enhance the sea breeze circulation. In three of the segments (segments two and three of 21-29 September, and segment one of 6-11 October) the one cycle per day peak weakened with height as a sub-diurnal two cycle per day peak intensified with height. Atkinson (1981) mentions that the diurnal sea breeze weakens with height. Also, the inversion height is noticeably shallower during these three segments (Figs. 7 and 9), and may be indicative of a less vertically developed sea breeze circulation.

D. ROTARY SPECTRA

There are different rotational patterns for each segment during the 8-12 September period. In segment one, the rotation changes from counterclockwise in level 1 to clockwise with height (Fig. 30). During segment two, the rotation is counterclockwise in every level (Fig. 31).

From 21-29 September, the segments again show differing rotational patterns. In segment one, the rotation changes from counterclockwise in level 1 to clockwise with height (Fig. 32). The trend in segment two is exactly the opposite; the rotation changes from clockwise in level 1 to counterclockwise with height (Fig. 33). In segment three there is counterclockwise rotation in the lower four levels,

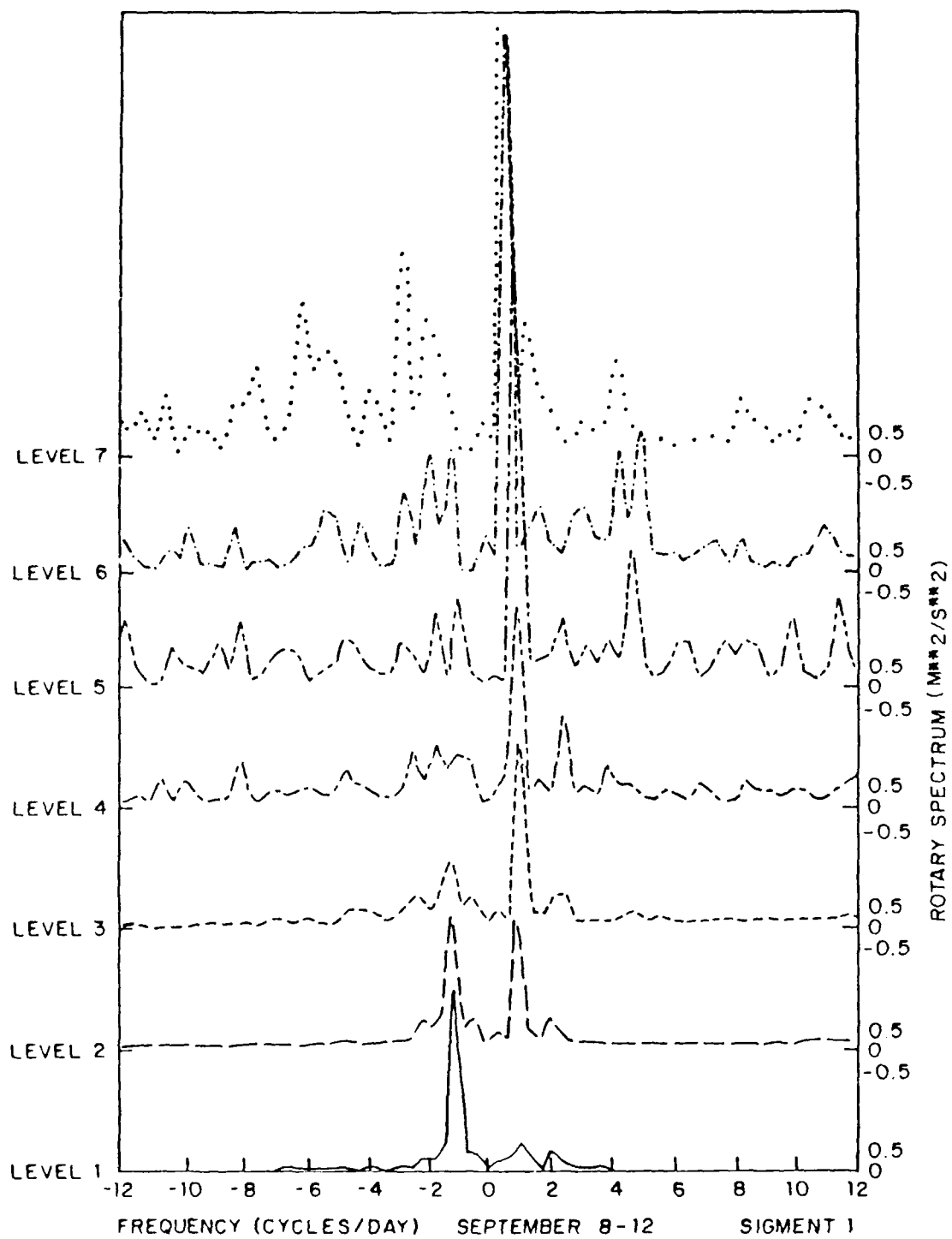


Figure 30. Rotary Spectrum (M^2/S^2)
September 8-12, 1985, Segment 1

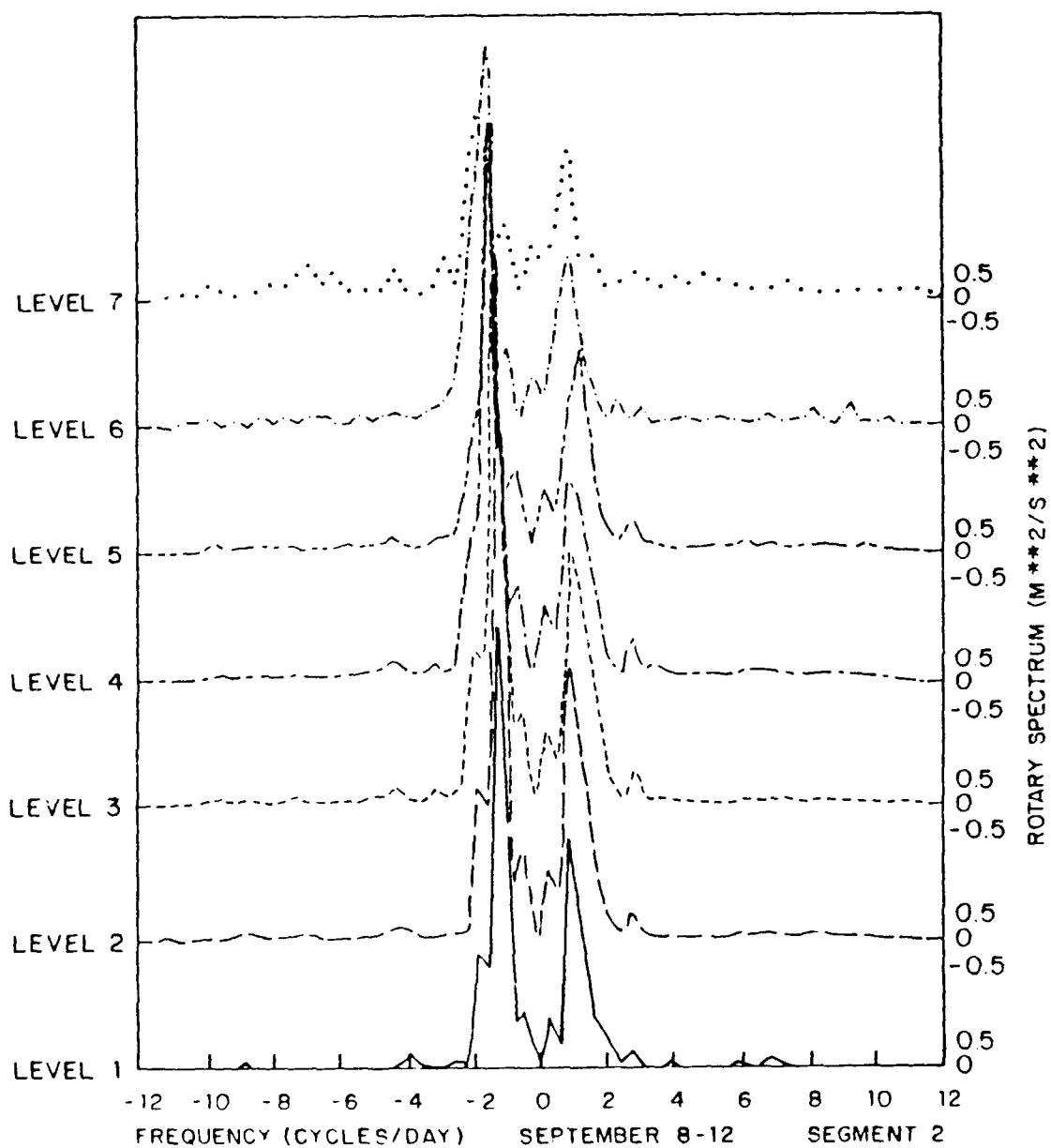
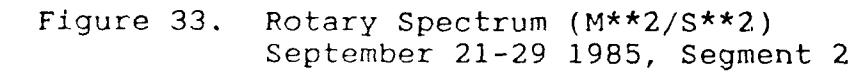


Figure 31. Rotary Spectrum (M^2/S^2)
September 8-12, 1985, Segment 2



but in levels 5, 6 and 7, there is too much noise in the data to determine the net rotation (Fig. 34).

In the 6-11 October period, each segment has a similar rotational pattern. Both segment one (Fig. 35) and segment two (Fig. 36) show changes in the rotation with height from clockwise to counterclockwise.

Overall, there appear to be three main trends in the rotary spectra analysis. First, there is a strong tendency for counterclockwise rotation in level 1. Six of the seven segments indicate counter-clockwise rotation at this level. Second, two of the segments show counterclockwise rotation in nearly every level. Third, above level 2 there is a strong tendency for clockwise rotation in most of the segments.

E. DISCUSSION OF RESULTS

The area in the Santa Barbara Channel where the sodar collected the data was dominated by sea and land breezes. The power density spectra analysis shows that considerably more energy is concentrated in the v-component than in the u-component and that most of the energy is centered near a frequency of one cycle per day, the frequency of the diurnal sea and land breeze circulations. Inspection of the time series of the v-component also reveals that a sea and land breeze was occurring on a daily basis. There are periods when the sea and land breezes undergo large increases in

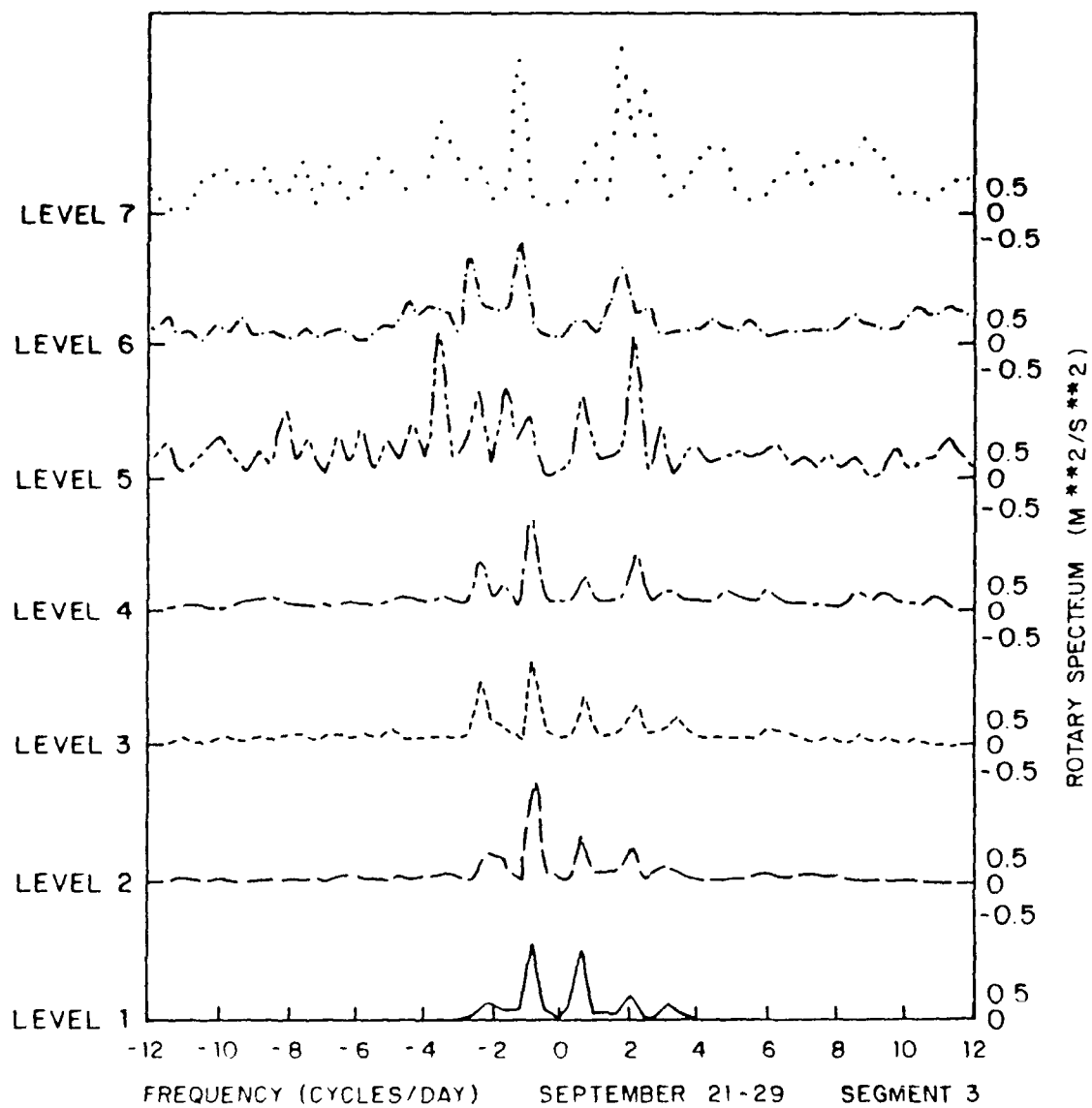


Figure 34. Rotary Spectrum (M^2/S^2)
September 21-29 1985, Segment 3

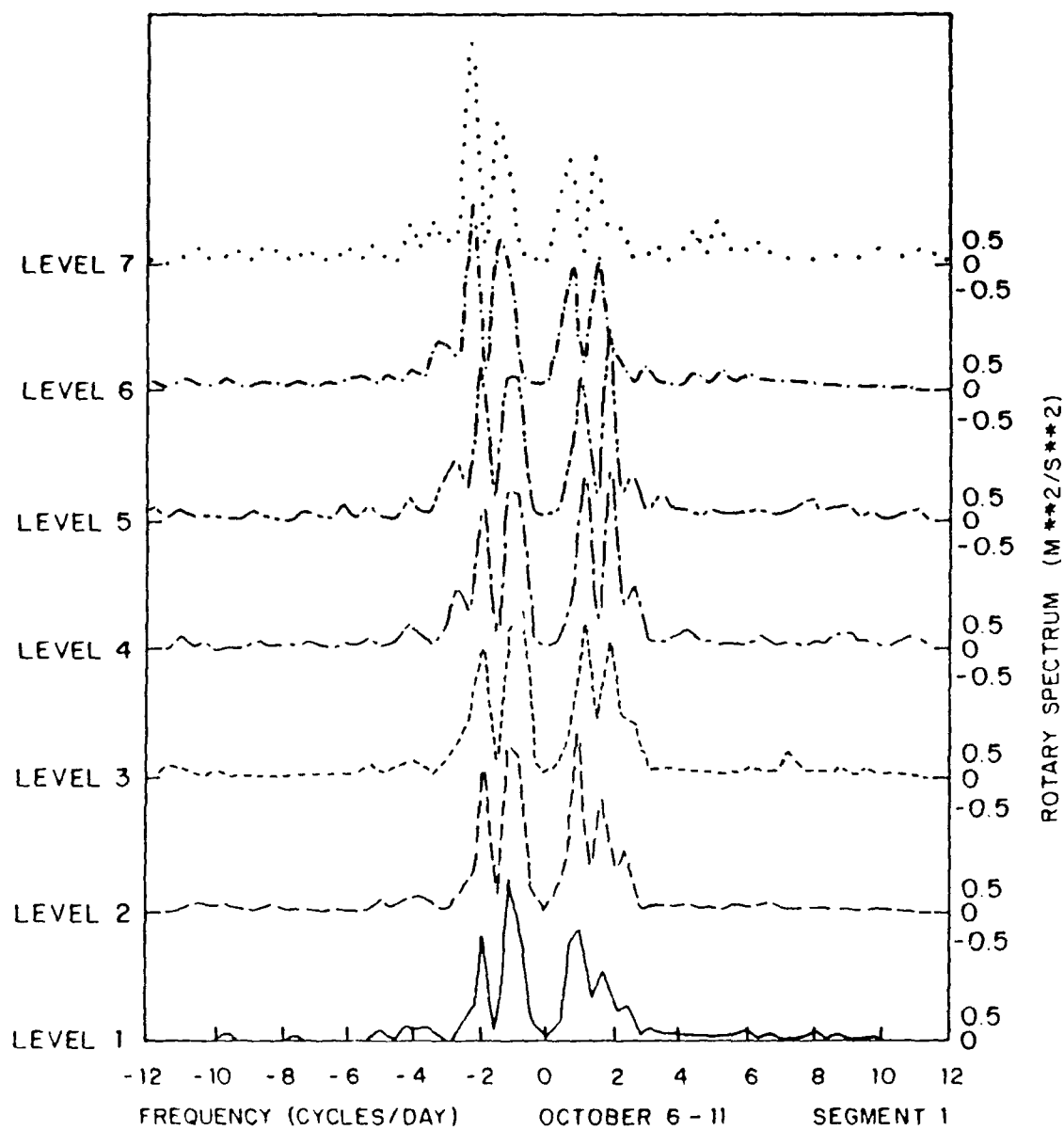


Figure 35. Rotary Spectrum (M^2/S^2)
October 6-11 1985, Segment 1

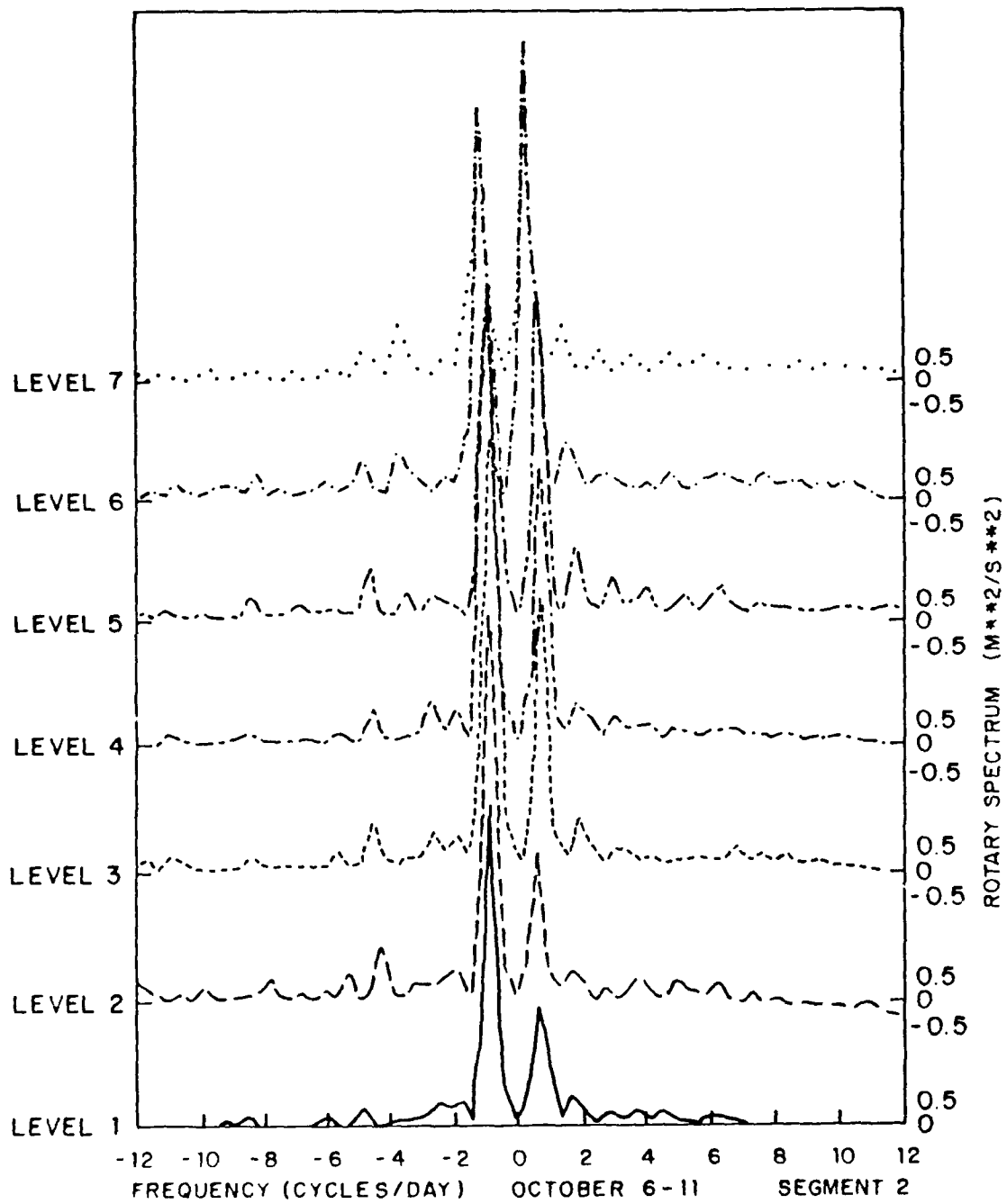


Figure 36. Rotary Spectrum (M^2/S^2)
October 6-11 1985, Segment 2

magnitude. These coincide with periods when the Santa Barbara Channel experienced cold frontal passages. However, many of the values for the northward and southward wind components are so large that it is unlikely they are due purely to sea and land breezes, respectively. Given the topography and geography of the Santa Barbara Channel region, it is likely that the sea and land breezes were not only enhanced by the cold frontal passages, but also by upslope and downslope winds.

Examination of time series of the horizontal wind components at each vertical level reveals three main features in the wind structure. During the morning there is an eastward wind component, in the afternoon there is a northward wind component and during the evening there is a southward wind component. During the morning, the predominant eastward component combines with northward or southward components, so the resultant wind in the morning ranges from north-eastward to south-southeastward. Likewise, the resultant wind during the afternoon ranges from northwestward to north-northwestward, and the resultant wind in the evening ranges from south-southwestward to southwestward. Inspection of time series of the data indicates the morning is a transition period between the evening land breezes and the afternoon sea breezes. In the morning there is a synoptically-driven eastward component,

when neither the sea or land breeze circulations have developed.

The rotary spectral analysis shows a strong tendency for counter-clockwise rotation in level 1 and in all of the levels for two segments. In the other five segments, the rotary spectra analysis indicates a strong tendency for clockwise rotation above level 2. The clockwise rotation of the sea breeze with time has been historically postulated by Haurwitz (1947), Frizzola and Fisher (1963), and Orlic et. al. (1988). Orlic et. al. (1988) state that sea breezes can rotate counterclockwise when modified by topographically induced flows.

The main secondary peak in the power density spectra analyses of the u and v wind components, in terms of number of occurrences and amount of energy, is the sub-diurnal peak at the two cycles per day frequency. The source of this persistent sub-diurnal peak may be related to the movement of the Gaviota Eddy or Catalina Eddy with time.

The regional topography along the northern part of the Santa Barbara Channel may have also influenced the wind recorded by the sodar station. The Santa Ynez mountains are oriented east-west and run parallel to the coast of the Santa Barbara Channel. The synoptically-driven northwesterly flow off the coast of southern California backs to westerly (eastward) in the Santa Barbara Channel, as it

reaches the western part of the Santa Ynez mountain range (Caldwell, et. al., 1986). The National Weather Service analyses presented earlier support this conclusion and eastward wind components observed in the time series of the u-component also support cyclonic turning of the wind around Point Arguello and Point Conception. This cyclonic turning of the wind leads to the formation of a cyclonic, mesoscale eddy in the lee of Point Conception, known as the Gaviota Eddy (Dabberdt, 1984). The power density spectra consistently indicate the presence of a sub-diurnal energy peak centered at or near two cycles per day, which may be attributable to the movement of the Gaviota Eddy over time.

IV. SUMMARY

A. REVIEW OF ANALYSIS PROCEDURES

Sodar wind data consisting of wind speeds and directions at 20 vertical levels have been analyzed to investigate the structure of the coastal atmospheric boundary layer. Wind variability is examined by using time series, synoptic weather analyses, power density spectra and rotary spectra. The data for this analysis were first prepared by converting the wind speed and direction data to east (u) and north (v) vector components. The data were then linearly extrapolated or interpolated, as appropriate, in space and time to produce unbroken time series at each of the 20 measurement altitudes from the surface to 525 meters.

The fast Fourier transform method was used as part of the data analysis, so it was necessary to detrend the data to avoid artificial data discontinuities and improve the statistical stability of frequency contributions to wind variability. A quadratic trend is removed to obtain mean and perturbation u and v component values from the original values. Power density spectra have been computed to investigate the strength and frequency of the sea and land breezes, the effect of frontal passages on the sea and land breezes, and the possible presence of sub-diurnal phenomena.

Rotary spectra are used to find rotational characteristics of the wind components at various frequencies and the possible effect of the rotation of the sea breeze circulation.

B. CONCLUSIONS

- The area around the sodar station was dominated by sea and land breezes, which occur on a daily basis.
- The northward and southward wind components are sea and land breezes, which are enhanced by cold frontal passages in the Santa Barbara Channel, and by topographic effects.
- Time series reveal three dominant wind components: morning eastward wind components, afternoon northward wind components and evening southward wind components.
- The morning eastward wind component appears to be synoptically-driven.
- There is a strong tendency for counterclockwise net rotation at an altitude of 25 meters and for clockwise net rotation above 50 meters.
- A persistent secondary peak at the sub-diurnal frequency of two cycles per day is evident in the power density spectra analysis.

C. AREAS FOR FUTURE RESEARCH

The sodar was located 10 meters away from a 30 meter high gap between two large bluffs. A meteorological tower was located 440 meters away from the shoreline at the seaward end of a pier, and thus was less affected by the shoreline topography. The wind data collected by the

meteorological tower's instruments are not used in this thesis, but a comparison of the wind data from the meteorological tower and the sodar station could provide insight into just how much of an effect the local topography had on the sodar wind data.

Another pertinent area for follow-on research would be to determine if there is a definite relationship between cyclonic mesoscale eddies such as the Gaviota Eddy or the Catalina Eddy, and cyclonic rotation of the wind in the vertical within the entire Santa Barbara Channel. A first step towards investigating a possible relationship would be to analyze the wind data from other sodar stations used during the SCCCAMP experiment, as they become available. Counterclockwise rotation is present in almost every segment at the lowest level, which is 25 meters above the surface. Also, two of the segments show counterclockwise rotation in almost every level. It has been suggested by other researchers that counterclockwise rotation of the sea breeze can result if the sea breeze is modified by topographically induced flows. An array of sodar stations surrounding the topography around the original sodar site at the head of the Ellwood pier would allow us to measure the net spatial rotation and gain a more complete understanding of the effects of local topography on sodar measurements below a height of 50 m.

To further our understanding and to develop an ability to predict the mesoscale wind structure, these questions need to be explored by observational studies using a data network dense enough to spatially and temporally resolve mesoscale wind variability. Numerical and theoretical studies are also needed to give additional physical insight into these questions.

LIST OF REFERENCES

- Arthur, R. S., 1965: On the Calculation of Vertical Motion in Eastern Boundary Currents from Determination of Horizontal Motion. *J. Geophys. Res.*, 70, 2799-2803.
- Atkinson, B. W., 1981: *Mesoscale Atmospheric Circulations*. Academic Press, Inc., 495 pp.
- Beach, J. B., 1980: Atmospheric Effects on Radio Wave Propagation. *Defense Electronics*, 12, 75-85.
- Bingham, C., M. D. Godfrey and J. W. Tukey, 1967: Modern Techniques of Power Spectrum Estimation. *IEEE Trans. on Audio and Electroacoustics*, AU-15, 2, 56-66.
- Caldwell, P. C., D. W. Stuart and K. H. Brink, 1986: Mesoscale Wind Variability near Point Conception, California during Spring 1983. *J. Clim. and Appl. Met.*, 25, 1241-1254.
- Chatfield, C., 1984: *The Analysis of Time Series*. Chapman and Hall, Inc., 246 pp.
- Dabberdt, W. F., 1984: Preliminary Experimental Design for the South Central Coast Cooperative Aerometric Monitoring Program. Interim Report, SRI International, 67 pp.
- Edinger, J. G., 1963: Modification of the Marine Layer over Coastal Southern California. *J. Appl. Met.*, 2, 706-712.
- Frizzola, J. A. and E. L. Fisher, 1963: A Series of Sea Breeze Observations in the New York City Area. *J. Appl. Met.*, 2, 722-739.
- Gill, A. E., 1982: *Atmospheric-Ocean Dynamics*. Academic Press, Inc., 662 pp.
- Halpern, D., 1974: Summertime Surface Diurnal Period Winds Measured over an Upwelling Region near the Oregon Coast. *J. Geophys. Res.*, 79, 2223-2230.
- Haurwitz, B., 1947: Comments on the Sea-Breeze Circulation. *J. Met.*, 4, 1-8.
- Holtslag, A. A. M. and F. T. M. Nieuwstadt, 1986: Scaling the Atmospheric Boundary Layer. *Boundary Layer Meteorology*, 36, 201-209.

Johnson, A., Jr. and J. J. O'Brien, 1973: A Study of an Oregon Sea Breeze Event. J. Appl. Met., 12, 1267-1283.

Little, C. G., 1969: Acoustic Methods for the Remote Probing of the Lower Atmosphere. Proc. IEEE, 57, 571-578.

Mastrantonio, G. and G. Fiocco, 1982: Accuracy of Wind Velocity Determinations with Doppler Sodars. Bull. Amer. Meteor. Soc., 21, 823-830.

McAllister, L. G., J. R. Pollard, A. R. Mahoney and P. J. R. Shaw, 1969: Acoustic Sounding: A New Approach to the Study of Atmospheric Structure. Proc. IEEE, 57, 579-587.

O'Brien, J. J. and R. D. Pillsbury, 1974: Rotary Wind Spectra in a Sea Breeze Regime. J. Appl. Met., 57, 820-825.

Olsson, L. E., W. P. Elliott and S. I. Hsu, 1973: Marine Air Penetration in Western Oregon: an Observational Study. Mon. Wea. Rev., 101, 356-362.

Orlic, M., B. Penzer and I. Penzer, 1988: Adriatic Sea and Land Breezes: Clockwise Versus Anticlockwise Rotation. J. Appl. Met., 27, 675-679.

Sethuraman, S. and G. S. Raynor, 1978: Comparison of the Mean Wind Speeds and Turbulence at a Coastal Site and an Offshore Location. J. Appl. Met., 19, 15-21.

Shaw, W. J., S. Borrmann, S. Fellbaum, C. E. Skupniewicz, C. A. Vaucher and G. T. Vaucher, 1986: Sodar, Rawinsonde and Surface Layer Measurements at a Coastal Site: SCCAMP Data Report, Part II. Technical Report, Naval Postgraduate School, 102 pp.

U. S. Navy (NAVAIR 50-1C-529), 1977: Marine Climatic Atlas of the World, v. 3, Government Printing Office, Washington, DC.

Wakimoto, R. M., 1987: The Catalina Eddy and its Effect on Pollution over Southern California. Bull. Amer. Meteor. Soc., 115, 837-855.

Wyckoff, R. J., D. W. Belan and F. F. Hall, Jr., 1973: A Comparison of the Low Level Radiosonde and the Acoustic Echo Sounder for Monitoring Atmospheric Stability. J. Appl. Met., 12, 1196-1204.

INITIAL DISTRIBUTION LIST

	No. copies
1. Defense Technical Information Center Cameron Station Alexandria, VA 22394-6145	2
2. Library, Code Naval Postgraduate School Monterey, CA 93943-5002	2
3. Associate Professor William J. Shaw Code 63Sr, Meteorology Department Naval Postgraduate School Monterey, CA 93943-5000	6
4. Professor Kenneth L. Davidson Code 63Ds, Meteorology Department Naval Postgraduate School Monterey, CA 93943-5000	1
5. Chairman, Code 63Rd Department of Meteorology Naval Postgraduate School Monterey, CA 93943-5000	1
6. Commander Naval Oceanography Command Bay St. Louis, Stennis Space Center, MS 39529-5001	1
7. Commanding Officer Naval Oceanographic Office Bay St. Louis Stennis Space Center, MS 39529-5001	1
8. Commanding Officer Naval Environmental Prediction Research Facility Monterey, CA 93943-5006	1
9. LCDR George M. Dunnavan, USN Department of Meteorology Naval Postgraduate School Monterey, CA 93943-5000	1

- | | |
|---|---|
| 10. LT Douglas H. Scovil, USN
5964 Margade Ave
Virginia Beach, VA 23462 | 2 |
| 11. Chairman,
Oceanography Department
U.S. Naval Academy
Annapolis, MD 21402 | 1 |
| 12. Chief of Naval Research
800 North Quincy St.
Arlington, VA 22217 | 1 |
| 13. Office of Naval Research
Code 420
Naval Ocean Research and Development Activity
800 N. Quincy St.
Arlington, VA 22217 | 1 |
| 14. Operations Analysis Programs
Code 30
Naval Postgraduate School
Monterey, CA 93943-5000 | 1 |